Journal of proteome research

pubs.acs.org/jpr

Article

Ex Vivo Equine Cartilage Explant Osteoarthritis Model: A Metabolomics and Proteomics Study

James R. Anderson,* Marie M. Phelan, Laura Foddy, Peter D. Clegg, and Mandy J. Peffers

Cite This: *J. Proteome Res.* 2020, 19, 3652−3667

Read Online

ACCESS | Metrics & More | Article Recommendations | Supporting Information

ABSTRACT: Osteoarthritis is an age-related degenerative musculoskeletal disease characterized by loss of articular cartilage, synovitis, and subchondral bone sclerosis. Osteoarthritis pathogenesis is yet to be fully elucidated with no osteoarthritis-specific biomarkers in clinical use. *Ex vivo* equine cartilage explants (n = 5) were incubated in tumor necrosis factor-α (TNF-α)/interleukin-1β (IL-1β)-supplemented culture media for 8 days, with the media removed and replaced at 2, 5, and 8 days. Acetonitrile metabolite extractions of 8 day cartilage explants and media samples at all time points underwent one-dimensional (1D) ^{1}H nuclear magnetic resonance metabolomic analysis, with media samples also undergoing mass spectrometry proteomic analysis. Within the cartilage, glucose and lysine were elevated following TNF-α/IL-1β treatment, while adenosine, alanine, betaine, creatine, myo-inositol, and uridine decreased. Within the culture media, 4, 4, and 6 differentially abundant metabolites and 154, 138, and 72 differentially abundant proteins were identified at 1−2, 3−5, and 6−8 days, respectively, including reduced alanine and increased isoleucine, enolase 1, vimentin, and lamin A/C following treatment. Nine potential novel osteoarthritis neopeptides were elevated in the treated media. Implicated pathways were dominated by those involved in cellular movement. Our innovative study has provided insightful information on early osteoarthritis pathogenesis, enabling potential translation for clinical markers and possible new therapeutic targets.

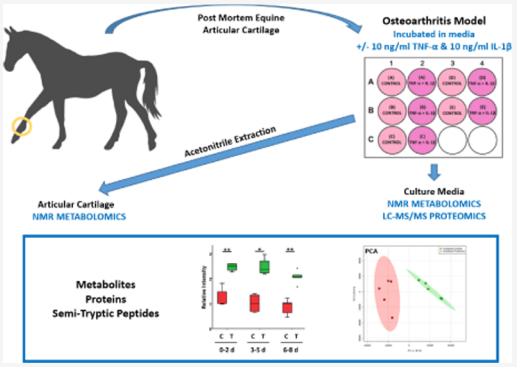

KEYWORDS: *osteoarthritis, cartilage, metabolomics, proteomics, nuclear magnetic resonance, mass spectrometry*

INTRODUCTION

Osteoarthritis (OA) is an age-related degenerative musculoskeletal disease characterized by loss of articular cartilage, synovial membrane dysfunction, abnormal bone proliferation, subchondral bone sclerosis, and altered biochemical and biomechanical properties.[1,2] For horses in the United Kingdom, OA is one of the leading welfare issues, resulting in substantial morbidity and mortality.[3,4] It is estimated that OA accounts for 60% of lameness seen in horses.[5] Within OA, extracellular matrix (ECM) degradation is driven by multiple matrix metalloproteinases (MMPs) and a disintegrin and metalloproteinases with thrombospondin motifs (ADAMTSs).[6] However, the underlying pathogenesis of OA is yet to be fully elucidated with no disease-modifying treatments currently available.[7,8] While a number of putative biomarkers have been identified for OA diagnosis in the horse, none are currently used within clinical practice.[9] Presently, equine OA is predominantly diagnosed through diagnostic imaging and clinical examination. However, due to the slow onset of the condition, this often leads to substantial pathology of the joint, particularly to articular cartilage prior to diagnosis.[10] There is therefore a need to develop diagnostic tests that are sensitive and specific to the early stages of OA, which are repeatable and reproducible, as well as gaining a greater understanding of the underlying pathogenesis.[11,12] Early detection of OA could enable timely management interventions, which could potentially slow the progression of the disease.

Tumor necrosis factor-α (TNF-α) and interleukin-1β (IL-1β) are both proinflammatory cytokines, which are central in OA pathogenesis.[13] TNF-α and IL-1β are secreted by mononuclear cells, synoviocytes, and articular cartilage and upregulate the gene expression of MMPs, ADAMTS-4, and ADAMTS-5, leading to significant ECM degradation.[14−16] Elevations in TNF-α and IL-1β are regularly identified within the OA synovial fluid (SF), including that of horses.[17−19] TNF-α and IL-1β have therefore become established experimental treatments for modeling OA pathology within *in vitro* and *ex vivo* studies, having been used both independently and as a combined treatment.[20−28]

Received: March 6, 2020
Published: July 23, 2020

Proteomics is the systematic, large-scale study of proteins within biological systems to assess the quantities, isoforms, modifications, structure, and function.[29] Previous studies have undertaken mass spectrometry (MS)-based proteomics using TNF-α and IL-1β OA models for secretome analysis of chondrocytes *in vitro* and *ex vivo* cartilage explants.[20−22,25] Results from these studies included increased media levels of MMPs, cartilage oligomeric matrix protein (COMP), aggrecan, and collagen VI.

During OA pathology, disease-associated peptide fragments (neopeptides) are generated from cartilage breakdown due to increased enzymatic activity/abundance of MMPs, ADAMTSs, cathepsins, and serine proteases.[30−32] MS analysis of these neopeptides can then be applied to identify potential early OA biomarkers.[33] Previously, a murine 32 amino acid peptide fragment, generated through increased activity of MMP and ADAMTS-4/5 and subsequent aggrecan degradation, was found to drive OA pain *via* Toll-like receptor 2.[34] Neopeptide targeting therefore has the potential to provide a localized analgesic at the site of joint degeneration.[33] Numerous equine OA studies investigating both synovial fluid (SF) and cartilage have identified potential neopeptides of interest.[30,35−37] Development of antibodies targeted to OA-specific neopeptides would provide the ability to monitor cartilage degeneration, assess therapeutic response, and potentially provide future novel therapeutic targets.[33,38]

Metabolomics uses a systematic methodology to comprehensively identify and quantify the metabolic profiles of biological samples.[39] ^{1}H nuclear magnetic resonance (NMR) metabolomics analysis provides a high level of technical reproducibility with a minimal level of sample preparation.[40] ^{1}H NMR analysis has previously been used to investigate OA in the SF of humans, horses, pigs, and dogs.[9,41−47] Synovial metabolites alanine, choline, creatine, and glucose have been identified as differentially abundant in OA across multiple studies and species.[9,41,43−46] NMR techniques have also previously been used to characterize the cartilage with high-resolution magical angle spinning (HRMAS) NMR utilized to assess the enzymatic degradation of bovine cartilage.[48−50] A guinea pig OA model using HRMAS NMR identified elevations in methylene resonances associated with chondrocyte membrane lipids and an increase in mobile methyl groups of collagen.[51] Another HRMAS NMR study of human OA cartilage identified a reduction in alanine, choline, glycine, lactate methyne, and *N*-acetyl compared to that of the healthy control cartilage.[52] However, no NMR studies to date have investigated the metabolic profile of culture media following the incubation of *ex vivo* cartilage within an OA model.

This is the first study to carry out ^{1}H NMR metabolomic analysis of extracted cartilage metabolites and to undertake ^{1}H NMR analysis of culture media using the TNF-α/IL-1β *ex vivo* OA cartilage model. Additionally, this is also the first study to use a multi-"omics" approach to simultaneously investigate the metabolomic profile of *ex vivo* cartilage and metabolomic/proteomic profiles of culture media using this OA model and conduct an integrated pathway analysis. It was hypothesized that following TNF-α/IL-1β treatment of *ex vivo* equine cartilage, ^{1}H NMR metabolomic and MS proteomic platforms would identify a panel of cartilage metabolites, which were able to differentiate the control from the treated cartilage and a panel of metabolites, proteins, and neopeptides within the associated culture media, which were differentially abundant at each tested time point of the early OA model.

METHODS

Equine *Ex Vivo* Cartilage Collection

A full-thickness cartilage was removed from all articular surfaces within five separate metacarpophalangeal joints of five 9-year-old mares of unknown breed within 24 h of slaughter at a commercial abattoir (F Drury and Sons, Swindon, U.K.). Cartilage samples were collected as a byproduct of the agricultural industry. The Animals (Scientific Procedures) Act 1986, Schedule 2, does not define collection from these sources as scientific procedures, and ethical approval was therefore not required. The cartilage collected from all joints was considered macroscopically normal with a score of 0 according to the OARSI histopathology initiative scoring system for horses[53] (Figure S1). The cartilage was washed in complete media containing Dulbecco's modified Eagle's medium (DMEM, 31885-023, Life Technologies, Paisley, U.K.) supplemented with 10% (v/v) fetal calf serum (FCS, Life Technologies), 5 μg/mL amphotericin B (Life Technologies), and 100 U/mL streptomycin and penicillin (Sigma-Aldrich, Gillingham, U.K.) (Figure S2).

The cartilage was dissected into 3 mm^2 sections and divided into two for each donor (control and treatment wells) on a 12-well plate (Greiner Bio-One Ltd., Stonehouse, U.K.). The explants were incubated for 24 h in complete media within a humidified atmosphere of 5% (v/v) CO_2 at 37 °C. The culture media was removed, the explants were washed in phosphate-buffered saline (PBS, Sigma-Aldrich), and replaced with the serum-free media (control) or serum-free media supplemented with 10 ng/mL TNF-α (PeproTech EC Ltd., London, U.K.) and 10 ng/mL IL-1β (R&D Systems Inc., Minneapolis, Minnesota) (treatment). After 48 h, the media was removed, centrifuged at 13 000*g*, 4 °C for 10 min, the supernatant was removed, and ethylenediaminetetraacetic acid (EDTA)-free protease inhibitor cocktail (Roche, Lewes, U.K.) was added to the cell-free media. The supernatant was then snap-frozen in liquid nitrogen and stored at −80 °C. The cartilage was washed in PBS, and control/treatment culture media was replaced as appropriate. Media collection was repeated at 5 and 8 days. After day 8, the cartilage was washed in PBS, weighed, snap-frozen in liquid nitrogen, and stored at −80 °C.

NMR Metabolomics

Cartilage Metabolite Extraction. Equal masses of cultured cartilage explants (in addition to three macroscopically normal equine cartilage samples, each divided into three to assess metabolite extraction reproducibility) were thawed out over ice and added to 500 μL of a 50:50 (v/v) ice-cold acetonitrile (ThermoFisher Scientific, Massachusetts): dd ^1H_2O and incubated on ice for 10 min. The samples were then sonicated using a microtip sonicator at 50 kHz and 10 nm amplitude in an ice bath for three 30 s periods and interspersed with 30 s rests (that ensured the extraction mixture temperature did not exceed 15 °C). The extraction mixture was then vortexed for 1 min and centrifuged at 12 000*g* for 10 min at 4 °C, and the supernatant was transferred before being snap-frozen in liquid nitrogen, lyophilized, and stored at −80 °C.[39]

Cartilage−NMR Sample Preparation. Each lyophilized sample was dissolved through the addition of 200 μL of 100 μM PO_4^{3-} pH 7.4 buffer (Na_2HPO_4, VWR International Ltd., Radnor, Pennsylvania; and NaH_2PO_4, Sigma-Aldrich) containing 100 μM trimethylsilyl propionate-d_4 (TSP, Sigma-Aldrich)

https://dx.doi.org/10.1021/acs.jproteome.0c00143
J. Proteome Res. 2020, 19, 3652−3667

and 1.2 μM sodium azide (NaN_3, Sigma-Aldrich) in 99.9% deuterium oxide (^2H_2O, Sigma-Aldrich). The samples were vortexed for 1 min and centrifuged at 12 000*g* for 2 min, and 190 μL of the supernatant was removed and transferred into 3 mm outer diameter NMR tubes using a glass pipette.

Culture Media−NMR Sample Preparation. The culture media was thawed over ice and centrifuged for 5 min at 21 000*g* and 4 °C. One hundred and fifty microliters of thawed culture media was diluted to a final volume containing 50% (v/v) culture media, 40% (v/v) dd ^1H_2O, 10% ^2H_2O, and 0.0025% (v/v) NaN_3, within an overall concentration of 500 mM PO_4^{3-} pH 7.4 buffer. The samples were vortexed for 1 min and centrifuged at 13 000*g* for 2 min at 4 °C, and 250 μL of the supernatant was removed and transferred to 3 mm outer diameter NMR tubes using a glass pipette.

NMR Acquisition. For each individual sample, one-dimensional (1D) ^{1}H NMR spectra, with the application of a Carr−Purcell−Meiboom−Gill (CPMG) filter to attenuate macromolecule (*e.g.*, proteins) signals, were acquired using the standard vendor pulse sequence cpmgpr1d on a 700 MHz NMR Bruker Avance III HD spectrometer with an associated TCI cryoprobe and a chilled Sample-Jet autosampler. All spectra were acquired at 25 °C, with a 4 s interscan delay, 256 transients for cartilage spectra and 128 transients for media spectra, with a spectral width of 15 ppm. Topsin 3.1 and IconNMR 4.6.7 software programs were used for acquisition and processing undertaking automated phasing, baseline correction, and a standard vendor processing routine (exponential window function with a 0.3 Hz line broadening). In addition to all cartilage extracts and culture media samples, protease inhibitor cocktail and treatment cytokines TNF-α and IL-1β were also analyzed separately to evaluate their metabolite profiles.

Metabolite Annotation and Identification. All acquired spectra were assessed to determine whether they met the minimum reporting standards (as outlined by the Metabolomics Society) prior to inclusion for statistical analysis.[54] These included appropriate water suppression, flat spectral baseline, and consistent line widths. Metabolite annotations and relative abundances were carried out using the Chenomx NMR Suite 8.2 (330-mammalian metabolite library). When possible, metabolite identifications were confirmed using 1D ^{1}H NMR in-house spectral libraries of metabolite standards. All raw 1D ^{1}H NMR spectra, together with annotated metabolite HMDB IDs and annotation level, are available within the EMBL-EBI MetaboLights repository (www.ebi.ac.uk/metabolights/MTBLS1495).[55] Quantile plots of 1D ^{1}H NMR spectra are shown in Figure S3.

Culture Media Proteomics

Protein Assay and StrataClean Resin Processing. Culture media was thawed over ice and centrifuged for 5 min at 21 000*g* and 4 °C. Media sample concentrations were determined using a Pierce 660 nm protein assay (Thermo Scientific, Waltham, Massachusetts). Fifty micrograms of protein for each sample was diluted with dd H_2O, producing a final volume of 1 mL. A StrataClean resin (10 μL) (Agilent, Santa Clara, California) was added to each sample, rotated for 15 min, and centrifuged at 400*g* for 1 min, and the supernatant was removed and discarded. The samples were then washed through the addition of 1 mL of ddH_2O, vortexed for 1 min, and centrifuged at 400*g* for 1 min, and the supernatant was removed and discarded. The wash step was repeated two further times.

Protein Digestion. One hundred and sixty microliters of 25 mM ammonium bicarbonate (Fluka Chemicals Ltd., Gillingham, U.K.) containing 0.05% (w/v) RapiGest (Waters, Elstree, Hertfordshire, U.K.) was added to each sample and heated at 80 °C for 10 min. DL-Dithiothreitol (Sigma-Aldrich) was added to produce a final concentration of 3 mM and incubated at 60 °C for 10 min, and then iodoacetamide (Sigma-Aldrich) was added (9 mM final concentration) and incubated at room temperature in the dark for 30 min. Two micrograms of proteomics-grade trypsin (Sigma-Aldrich) was added to each sample and rotated at 37 °C for 16 h, and trypsin treatment was then repeated for a 2 h incubation. The samples were centrifuged at 1000*g* for 1 min, the digest was removed, trifluoroacetic acid (TFA, Sigma-Aldrich) was added (0.5% (v/v) final concentration), and rotated at 37 °C for 30 min. Finally, the digests were centrifuged at 13 000*g* and 4 °C for 15 min, and the supernatant was removed and stored at 4 °C.

Label-Free LC-MS/MS. All media digests were randomized and individually analyzed using liquid chromatography-tandem mass spectrometry (LC-MS/MS) on an UltiMate 3000 Nano LC System (Dionex/Thermo Scientific) coupled to a Q Exactive Quadrupole-Orbitrap instrument (Thermo Scientific). Full LC-MS/MS instrument methods are described in the Supporting Information. Tryptic peptides, equivalent to 250 ng of protein, were loaded onto the column and run over a 1 h gradient, interspersed with 30 min blanks (97%, v/v) high-performance liquid chromatography grade H_2O (VWR International), 2.9% acetonitrile (Thermo Scientific), and 0.1% TFA. In addition to individual time points, the pooled samples for control and treatment groups were also analyzed to investigate the differences in the overall secretome. The mass spectrometry proteomics data have been deposited to the ProteomeXchange Consortium *via* the PRIDE partner repository with the data set identifiers PXD017153 and 10.6019/PXD017153.[56] Representative ion chromatograms are shown in Figure S4.

LC-MS/MS Spectra Processing and Protein Identification. Spectral alignment, peak picking, total protein abundance normalization, and peptide/protein quantification were undertaken using Progenesis QI 2.0 (Nonlinear Dynamics, Waters). The exported top 10 spectra for each feature were then searched against the *Equus caballus* database for peptide and protein identifications using PEAKS Studio 8.5 (Bioinformatics Solutions Inc., Waterloo, Ontario, Canada) software. Search parameters were as follows: precursor mass error tolerance, 10.0 ppm; fragment mass error tolerance, 0.01 Da; precursor mass search type, monoisotopic; enzyme, trypsin; maximum missed cleavages, 1; nonspecific cleavage, none; fixed modifications, carbamidomethylation; and variable modifications, oxidation or hydroxylation and oxidation (methionine). A filter of a minimum of two unique peptides was set for protein identification and quantitation with a false discovery rate (FDR) of 1%.

One-Dimensional Sodium Dodecyl Sulfate Polyacrylamide Gel Electrophoresis (1D SDS PAGE). Media samples for each donor were combined for all time points and analyzed *via* one-dimensional sodium dodecyl sulfate polyacrylamide gel electrophoresis (1D SDS PAGE). One microgram of each sample was added to the Laemmli loading buffer Novex (Thermo Scientific) producing a final concen-

https://dx.doi.org/10.1021/acs.jproteome.0c00143
J. Proteome Res. 2020, 19, 3652−3667

Table 1. Metabolites Annotated within the Cartilage and Culture Media Using Chenomx[a]

database identifier	metabolite identification	cartilage	cartilage reliability	media	media reliability
HMDB00695	2-oxoisocaproate			Y	MS level 2
HMDB00491	3-methyl-2-oxovalerate			Y	MS level 2
HMDB31645	acetamide	Y	MS level 2		
HMDB00042	acetate[b]	Y	MS level 1	Y	MS level 1
HMDB01659	acetone[b]			Y	MS level 2
HMDB00050	adenosine	Y	MS level 2		
HMDB00517	arginine			Y	MS level 2
HMDB00191	aspartate	Y	MS level 1		
HMDB00043	betaine	Y	MS level 1		
HMDB00097	choline			Y	MS level 1
HMDB00094	citrate	Y	MS level 1	Y	MS level 1
HMDB00064	creatine	Y	MS level 1		
HMDB00562	creatinine	Y	MS level 1	Y	MS level 1
HMDB00192	cystine			Y	MS level 2
HMDB00122	D-glucose	Y	MS level 1		
HMDB04983	dimethyl sulfone	Y	MS level 2		
HMDB00108	ethanol[b]			Y	MS level 1
HMDB00142	formate[b]	Y	MS level 2	Y	MS level 2
HMDB00123	glycine	Y	MS level 1	Y	MS level 1
HMDB00870	histamine			Y	MS level 2
HMDB00172	isoleucine	Y	MS level 1	Y	MS level 1
HMDB00863	isopropanol[b]			Y	MS level 2
HMDB00190	lactate[b]	Y	MS level 1	Y	MS level 1
HMDB00161	L-alanine	Y	MS level 1	Y	MS level 1
HMDB00062	L-carnitine			Y	MS level 2
HMDB00148	L-glutamate	Y	MS level 1	Y	MS level 1
HMDB00641	L-glutamine	Y	MS level 1	Y	MS level 1
HMDB00177	L-histidine			Y	MS level 1
HMDB00687	L-leucine	Y	MS level 1	Y	MS level 1
HMDB00159	L-phenylalanine	Y	MS level 1	Y	MS level 1
HMDB00167	L-threonine	Y	MS level 2	Y	MS level 2
HMDB00158	L-tyrosine	Y	MS level 1	Y	MS level 1
HMDB00883	L-valine	Y	MS level 1	Y	MS level 1
HMDB00182	lysine	Y	MS level 1	Y	MS level 1
HMDB00765	mannitol[b]			Y	MS level 1
HMDB01875	methanol[b]			Y	MS level 2
HMDB00696	methionine	Y	MS level 1	Y	MS level 1
HMDB01844	methylsuccinate	Y	MS level 2		
HMDB00211	myo-Inositol	Y	MS level 1		
HMDB03269	nicotinurate	Y	MS level 2	Y	MS level 2
HMDB00895	*O*-acetylcholine	Y	MS level 2		
HMDB00210	pantothenate	Y	MS level 2		
HMDB00267	pyroglutamate			Y	MS level 2
HMDB00243	pyruvate	Y	MS level 1		
HMDB00086	*sn*-glycero-3-phosphocholine	Y	MS level 2		
HMDB00254	succinate[b]	Y	MS level 1	Y	MS level 1
HMDB00929	tryptophan			Y	MS level 1
HMDB00300	uracil	Y	MS level 2		
HMDB00296	uridine	Y	MS level 1		
HMDB00001	τ-methylhistidine	Y	MS level 2		

[a]Metabolites additionally identified using a 1D ^{1}H NMR in-house library have been assigned to the Metabolomics Standards Initiative (MSI) level 1. Y = yes.[60] [b]Metabolites removed from subsequent analyses.

tration of 15% glycerine, 2.5% SDS, 2.5% tris(hydroxymethyl)-aminomethane, 2.5% HCL, and 4% β-mercaptoethanol at pH 6.8 and heated at 95 °C for 5 min. The samples were loaded onto a 4−12% Bis−Tris polyacrylamide electrophoresis gel (NuPAGE Novex, Thermo Scientific), and protein separation was carried out at 200 V for 30 min at room temperature. Protein bands were visualized *via* silver staining (Thermo Scientific) following the manufacturer's instructions. Gel images were converted to 8-bit grayscale, and protein band intensities were analyzed using densitometry with the software ImageJ (NIH, Bethesda, Maryland).

Semitryptic Peptide Identification. To identify potential neopeptides, a "semitryptic" search was undertaken. The same PEAKS search parameters were used for protein identification,

https://dx.doi.org/10.1021/acs.jproteome.0c00143
J. Proteome Res. 2020, 19, 3652−3667

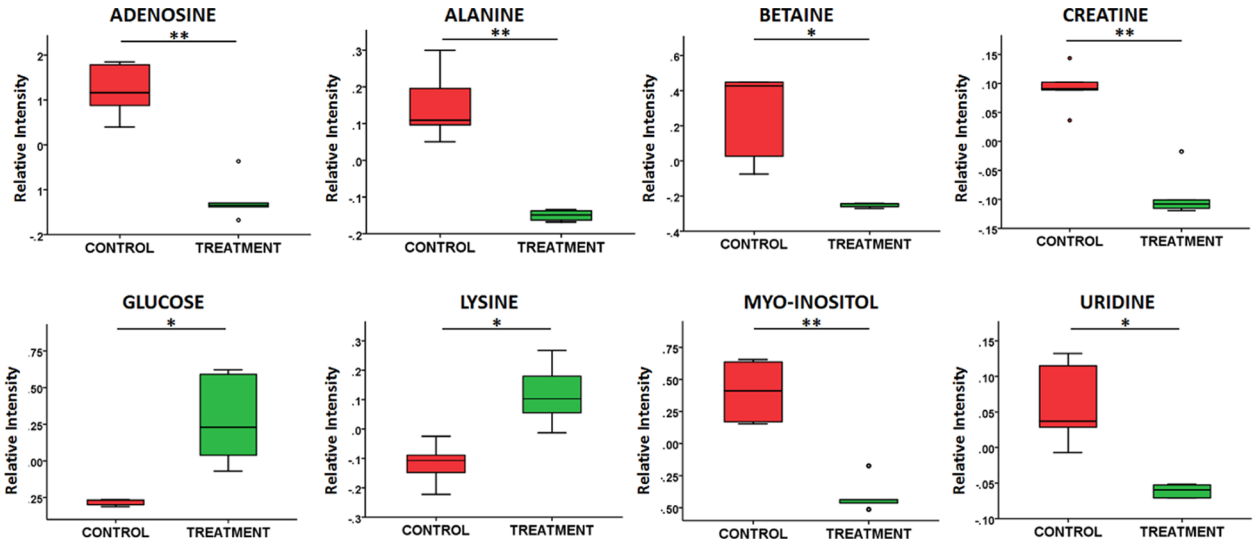

Figure 1. Boxplots of differentially abundant extracted *ex vivo* equine cartilage metabolites for control (n = 5) and following TNF-α/IL-1β treatment (n = 5), shown as relative intensities. t-Test: * = $p < 0.05$ and ** = $p < 0.01$.

with the exception that "nonspecific cleavage" was altered from "none" to "one". The "peptide ion measurements" file was then exported and analyzed using the online neopeptide analyzer software tool.[38]

Statistical Analysis

Cartilage metabolite profiles were normalized using probabilistic quotient normalization (PQN).[57] Media metabolites were normalized to the TSP concentration, and protein profiles were normalized to total ion current (TIC). Prior to multivariate analysis, metabolite and protein profiles were Pareto-scaled.[58] MetaboAnalyst 3.5 (http://www.metaboanalyst.ca) was used to produce principal component analysis (PCA) plots and provide principal component 1 (PC1) loading magnitude values. t-Tests were carried out using MetaboAnalyst 3.5 (protein and metabolite abundances) and the neopeptide analyzer (neopeptides) with $p < 0.05$ (and a fold change of >2 for proteins) considered statistically significant. The Benjamini−Hochberg false discovery rate method was applied for the correction of multiple testing.[59] The SPSS 24 software package was used to produce all boxplots and PC1 loading magnitude graphs.

Pathway Analysis

Owing to the minimal annotation of the equine genome, equine proteins and metabolites were converted to their human orthologues prior to pathway analysis. Functional analyses of differentially expressed proteins and metabolites within the culture media were undertaken to evaluate the differences due to the application of TNF-α and IL-1β at all three time points. Networks, functional analyses, and canonical pathways were generated through the use of ingenuity pathway analysis (IPA, Ingenuity Systems, Redwood City, California) on the list of differentially expressed proteins and metabolites, $p < 0.05$. Protein and metabolite symbols were used as identifiers, and the Ingenuity Knowledge Base gene was used as a reference for pathway analysis. These molecules were overlaid onto a global molecular network contained in the Ingenuity Knowledge Base. Networks of network-eligible molecules were algorithmically generated based on their connectivity. The functional analyses identified the biological functions and diseases that were most significant to the data set. A right-tailed Fisher's exact test was used to calculate the p values. Canonical pathway analyses identified pathways from the IPA library of canonical pathways that were most significant to the data sets.

RESULTS

NMR Metabolomics

Protease Inhibitor Cocktail, TNF-α, and IL-1β Metabolite Profiles. Protease inhibitor cocktail was found to have high levels of mannitol, and thus this metabolite was removed from all analyses. Within the spectral profiles of TNF-α and IL-1β acquired separately, the metabolites acetate, acetone, ethanol, formate, lactate, methanol, and succinate were identified. These metabolites were therefore also removed from further analyses.

Analysis of Cartilage Metabolites. Acetonitrile metabolite extraction was identified to be highly reproducible with technical replicates clustering within a PCA plot for three separate macroscopically normal cartilage samples (Figure S5). In total, 35 metabolites were identified within the equine cartilage (Table 1). Of these, following the removal of metabolites previously mentioned, eight were identified as being differentially abundant between the control and treatment groups (Figure 1). Glucose and lysine levels were elevated following TNF-α/IL-1β treatment, while adenosine, alanine, betaine, creatine, myo-inositol, and uridine levels decreased. PCA identified that metabolite profiles separated into two distinct clusters, separating the control and treatment groups (Figure 2A). Of the top 25 PC1 loadings, myo-inositol was found to be the most influential cartilage metabolite in separating the control and treated samples, followed by glucose, betaine, and alanine (Figure 2B).

Analysis of Media Metabolites. Spectral quality control *via* metabolomics standard initiative identified two samples that failed due to salt precipitation and as such were removed from further analyses.[54,61] Following metabolite identification and quantification, one sample was identified as an outlier and subsequently removed from statistical analyses. Isopropanol was identified within all media samples. As this was considered a likely contaminant during cartilage culture, together with

https://dx.doi.org/10.1021/acs.jproteome.0c00143
J. Proteome Res. 2020, 19, 3652−3667

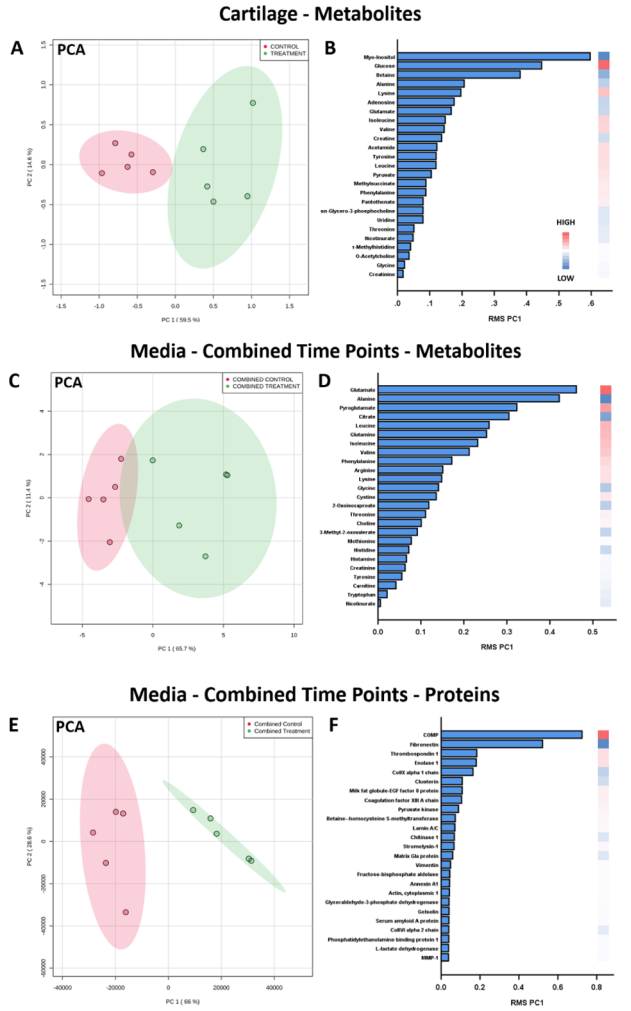

Figure 2. PCA (A, C, E), and principal component 1 root-mean-square (PC1 RMS) values (B, D, F) for the 25 components with the highest magnitude for metabolites and proteins present in *ex vivo* equine cartilage and culture media for combined time points over 8 days, comparing controls (red, n = 5) to TNF-α/IL-1β treatment (green, n = 5). RMS: high = high in treatment with respect to control; low = low in treatment with respect to control.

metabolites previously mentioned, isopropanol was also removed from all analyses. In total, 34 metabolites were identified within the culture media (Table 1). Time points were analyzed separately with four, four, and six metabolites identified as being differentially abundant between the control and treatment groups for 1−2, 3−5, and 6−8 days time points, respectively (Figure 3). Choline levels were increased in the treated samples compared to those in controls for all three time points, while alanine and citrate levels decreased. At 3−5 days, glutamate levels were reduced following treatment. At 6−8 days, following treatment, arginine and isoleucine levels were elevated, while 2-oxoisocaproate and 3-methyl-2-oxovalerate levels were found to decrease. PCA of combined and separated time points identified a clear separation between the metabolite profiles of the control and treated media samples (Figures 2C and 4A−C). Metabolite loadings for PC1 indicate that this separation is driven primarily by alanine and glutamate (Figure 2D).

LC-MS/MS Proteomics

Analysis of Media Proteins. In total, 303 proteins were identified within the analyzed culture media samples (Table S1). When time points were analyzed separately, 154, 138, and 72 proteins were identified as being differentially abundant, with >2-fold change, between the control and treatment groups for 1−2, 3−5, and 6−8 days time points, respectively. PCA analysis of the combined protein profiles identified groups that were primarily separated by an elevated COMP and decreased fibronectin following treatment (Figure 2E,F). PCA multivariate analysis also identified a clear discrimination between the control and treatment groups at all three time points (Figure 4D−F). At each separated time point, the PC1 loadings with the 25 greatest magnitudes corresponding to individual proteins were identified (Figure S6). Boxplots in Figure 5 represent proteins that were found to be represented within the top 25 PC1 loading magnitudes at all three time points (coagulation factor XIII A chain, COMP, enolase 1, lamin A/C, and MMP-3) and extracellular matrix-related proteins of interest represented at 2/3 time points (collagen type VI α 2 chain, collagen type X α 1 chain, fibromodulin, fibronectin, matrix Gla protein, MMP-1, and vimentin). Coagulation factor XIII A chain, enolase 1, and lamin A/C were elevated at all three time points following treatment. MMP-1 and MMP-3 levels were found to be statistically elevated at 0−2 days only. Fibromodulin and vimentin levels were increased following treatment at both 0−2 and 3−5 days time points, while COMP levels increased at 0−2 and 6−8 days. Collagen type VI α 2 chain and matrix Gla protein levels decreased following treatment at 3−5 and 6−8 days, while collagen type X α 1 chain and fibronectin levels statistically decreased at 6−8 days alone.

Silver stain analysis of the media profiles for combined time points identified two protein bands that were decreased in abundance following TNF-α/IL-1β treatment, with molecular weights of 160−260 and 260 kDa (Figure S7).

Semitryptic Peptides. PCA of all identified semitryptic peptides within the combined control and combined treated samples identified far less variation within the treatment group (Figure 6). This was also identified for all time points analyzed individually (Figure S8). In total, nine potential novel OA neopeptides were identified, which were elevated in the treated media samples (Table 2). These included semitryptic peptides of extracellular matrix proteins aggrecan, cartilage intermediate layer protein, collagen type VI α 2 chain, and vimentin.

Pathway Analysis

Pathways implicated within the model at time points 0−2 and 3−5 days following TNF-α/IL-1β treatment were largely dominated by those involved in cellular movement (Figure S9). These included the upregulation of the canonical pathways actin cytoskeleton signaling (0−2 days, $p = 4.37 \times 10^{-9}$; 3−5 days, $p = 9.77 \times 10^{-4}$), RhoA (Ras homologue gene family A) signaling (0−2 days, $p = 1.45 \times 10^{-8}$; 3−5 days, $p = 4.47 \times 10^{-4}$), and signaling by Rho family GTPases (0−2 days, $p = 1.29 \times 10^{-7}$; 3−5 days, $p = 2.69 \times 10^{-4}$) at both time points and the upregulation of actin-based motility by Rho ($p = 1.95 \times 10^{-8}$) at 0−2 days (Figure 7). Network analysis of cellular movement, migration, and invasion at 0−2 days identified key contributors to these pathways to include both metabolites and proteins, including increased levels of L-glutamate, vimentin, coagulation factor XIII A chain, fibromodulin, lamin A/C, and enolase 1 and reduced levels

https://dx.doi.org/10.1021/acs.jproteome.0c00143
J. Proteome Res. 2020, 19, 3652−3667

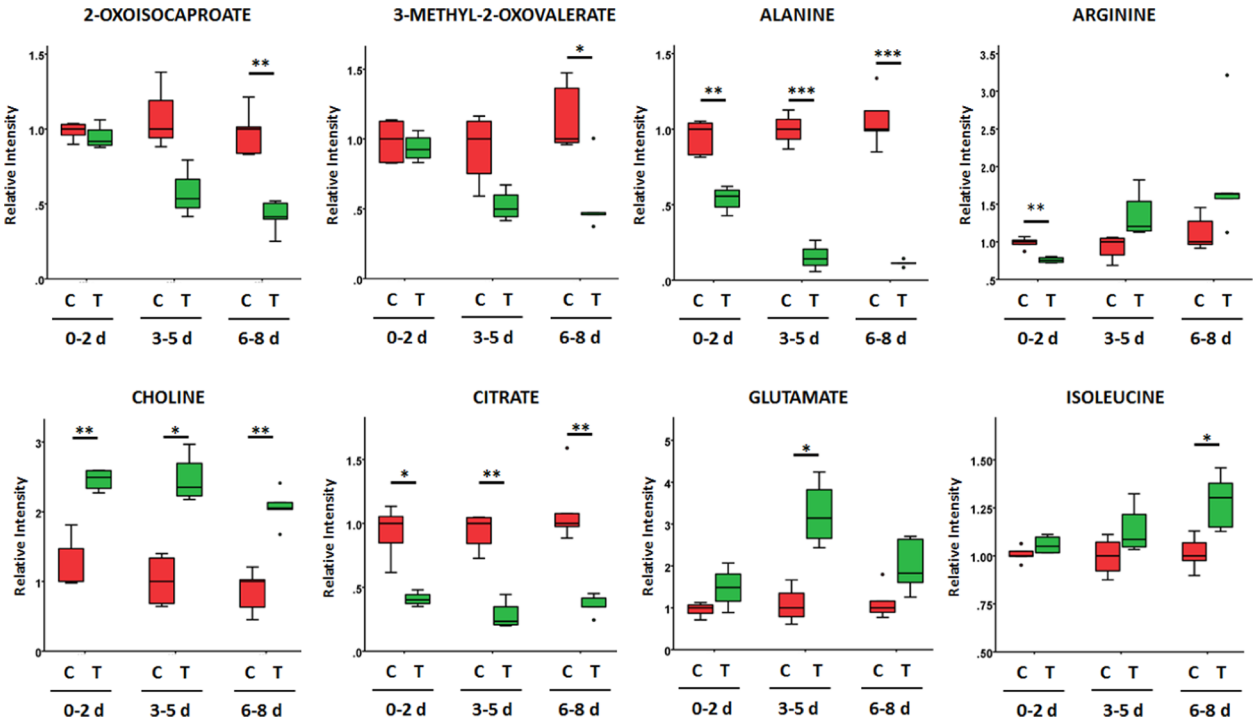

Figure 3. Boxplots of differentially abundant metabolites within the culture media following incubation of *ex vivo* equine cartilage for control samples (C, red) and following TNF-α/IL-1β treatment (T, green), at 0−2, 3−5, and 6−8 days (d). Metabolite abundances are shown as relative intensities. *t*-Test: * = $p < 0.05$, ** = $p < 0.01$, and *** = $p < 0.001$. Control ($n = 5$) and TNF-α/IL-1β treatment ($n = 5$) for each separate time point.

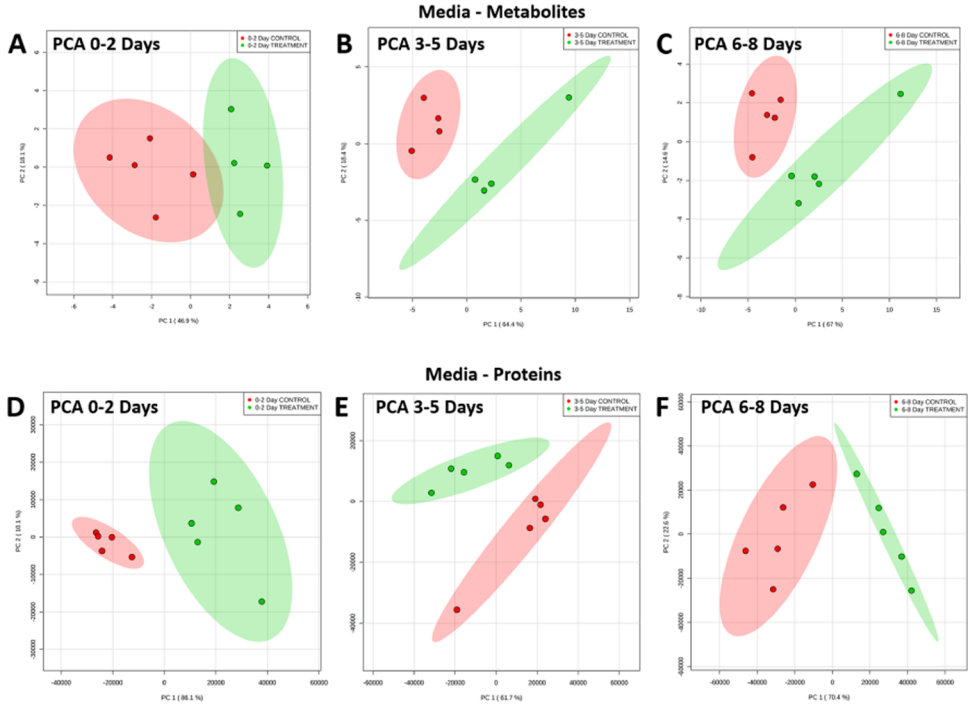

Figure 4. Principal component analysis (PCA) plots of media metabolite (A−C) and protein (D−F) profiles at 0−2, 3−5, and 6−8 days for controls (green, $n = 5$) and TNF-α/IL-1β treatment (red, $n = 5$) of *ex vivo* equine cartilage.

of fibrillin 1, tissue inhibitor of metalloproteinases 2, and collagen type XI α 1 chain following treatment (Figure S10).

Glycolysis was also identified as being upregulated at both 0−2 days ($p = 3.89 \times 10^{-7}$) and 3−5 days ($p = 6.92 \times 10^{-8}$) (Figure 7). For 6−8 days, pathway directionality was unable to be obtained for any of the significant pathways identified. Alanine degradation and biosynthesis pathways were identified as significant for both 3−5 days (alanine biosynthesis II, $p = 3.80 \times 10^{-4}$; alanine degradation III, $p = 3.80 \times 10^{-4}$) and 6−8 days (alanine biosynthesis II, $p = 8.51 \times 10^{-3}$; alanine biosynthesis III, $p = 4.27 \times 10^{-3}$; alanine degradation III, $p = 8.51 \times 10^{-3}$).

https://dx.doi.org/10.1021/acs.jproteome.0c00143
J. Proteome Res. 2020, 19, 3652−3667

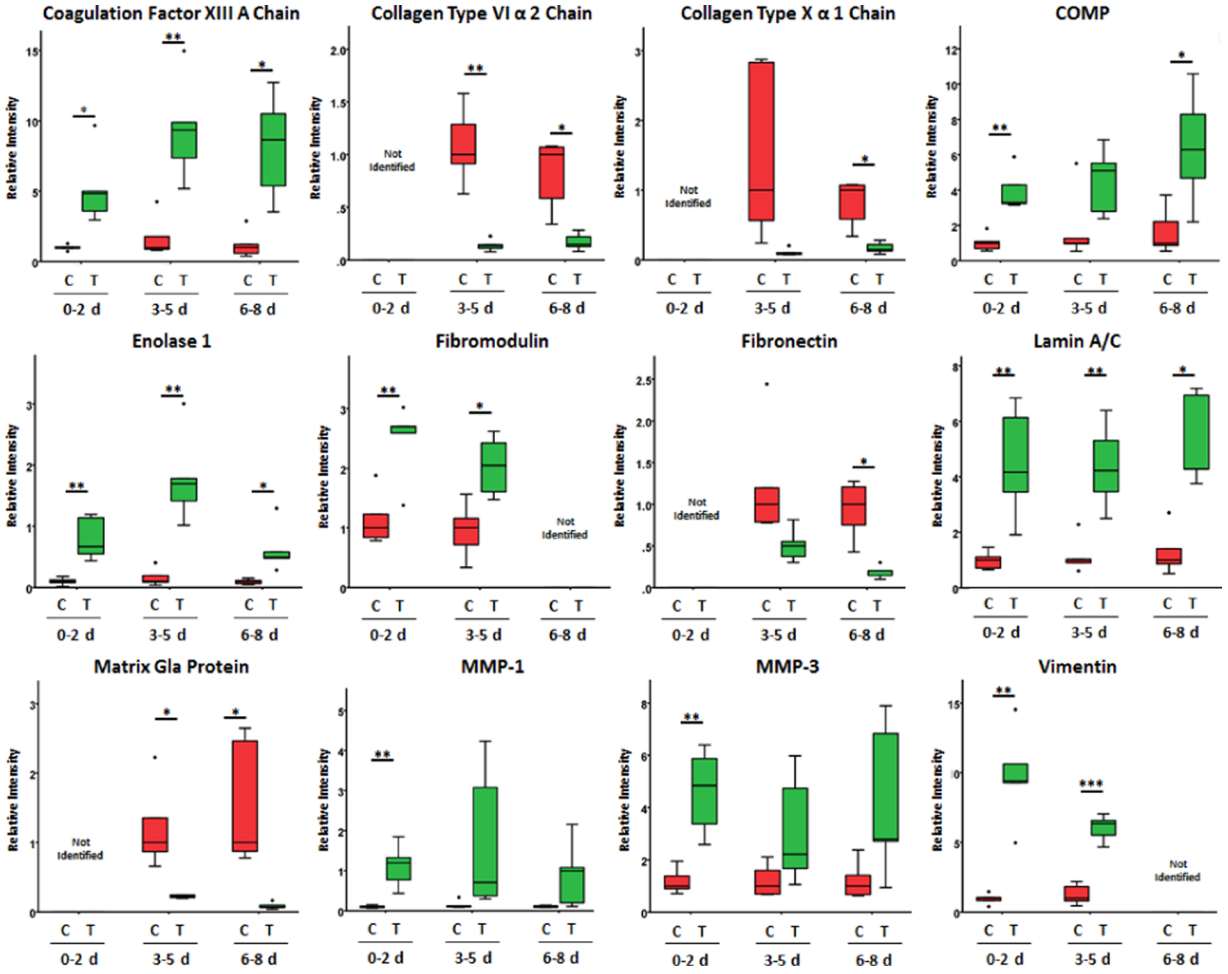

Figure 5. Boxplots of differentially abundant proteins within the culture media following incubation of *ex vivo* equine cartilage for control samples (C, red) and following TNF-α/IL-1β treatment (T, green), at 0−2, 3−5, and 6−8 days (d). Protein abundances are shown as relative intensities. *t*-Test: * = $p < 0.05$, ** = $p < 0.01$, and *** = $p < 0.001$. Control ($n = 5$) and TNF-α/IL-1β treatment ($n = 5$) for each separate time point.

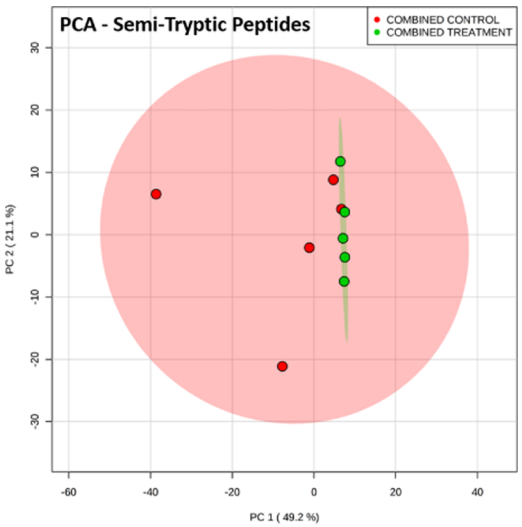

Figure 6. Principal component analysis (PCA) of semitryptic peptide profiles within the culture media of control (red, $n = 5$) and TNF-α/IL-1β-treated (green, $n = 5$) *ex vivo* equine cartilage. Time points pooled for each individual donor.

DISCUSSION

In this study, TNF-α/IL-1β treatment of *ex vivo* equine cartilage explants was used to model early OA to gain a greater understanding of OA pathogenesis and identify potential OA markers. ^{1}H NMR metabolomic and LC-MS/MS proteomic analyses of culture media at 0−2, 3−5, and 6−8 days were undertaken. In addition, the ^{1}H NMR metabolomic analysis of acetonitrile-extracted cartilage metabolites (following 8 days of incubation) was also carried out.

Within culture media, following TNF-α/IL-1β treatment, elevations in endopeptidases MMP-1 and MMP-3 at 0−2 days, with a similar trend at both other time points, were identified as expected.[62] Elevated MMP-1 activity has previously been identified within equine OA SF, with the general MMP activity also found to be correlated to the severity of cartilage damage.[63,64] Also, as previously reported, elevations in the noncollagenous ECM protein COMP were also identified within the TNF-α/IL-1β equine OA model, with COMP considered a marker of cartilage breakdown.[65,66] Clinically, elevated COMP levels have been identified within human OA SF, although within equine OA, one study identified reduced levels with COMP levels being unable to stage the disease.[67,68] Fibronectin was identified as a key discriminator between the control and treatment groups with reduced secreted fibronectin identified within the media following TNF-α/IL-

https://dx.doi.org/10.1021/acs.jproteome.0c00143
J. Proteome Res. 2020, 19, 3652−3667

Table 2. Potential Osteoarthritis Neopeptides[a]

time point	protein	accession number	neopeptide sequence	previous amino acid	following amino acid	fold change	*p*-value
0–2 days	aggrecan	F7C3C6	TYGVRPSSETYDVY	R	C	3.6	7.76×10^{-5}
3–5 days	cartilage intermediate layer protein	F7C2J3	AIGVPQPYLNK	N	L	2.2	1.83×10^{-4}
	unknown	N/A	NGPTESTFSTSWK	C	G	5.4	2.24×10^{-4}
	unknown	N/A	LVIIR	N	K	4.9	3.05×10^{-4}
	vimentin	F7B5C4	RQVDQLTNDK	L	A	2.7	4.09×10^{-4}
combined	unknown	N/A	AFDQLR	H	N	6.4	3.05×10^{-4}
	collagen type VI α 2 chain	F7CGV8	KQNVVPTVVAV	R	G	6.5	3.85×10^{-4}
	unknown	N/A	DGAFLLR	E	Q	11.7	4.10×10^{-4}
	unknown	N/A	SILGVR	M	S	5.6	4.61×10^{-4}

[a]Semitryptic peptides of the extracellular matrix-related and unknown proteins, identified within the culture media, with an increased abundance following TNF-α/IL-1β treatment of *ex vivo* equine cartilage.

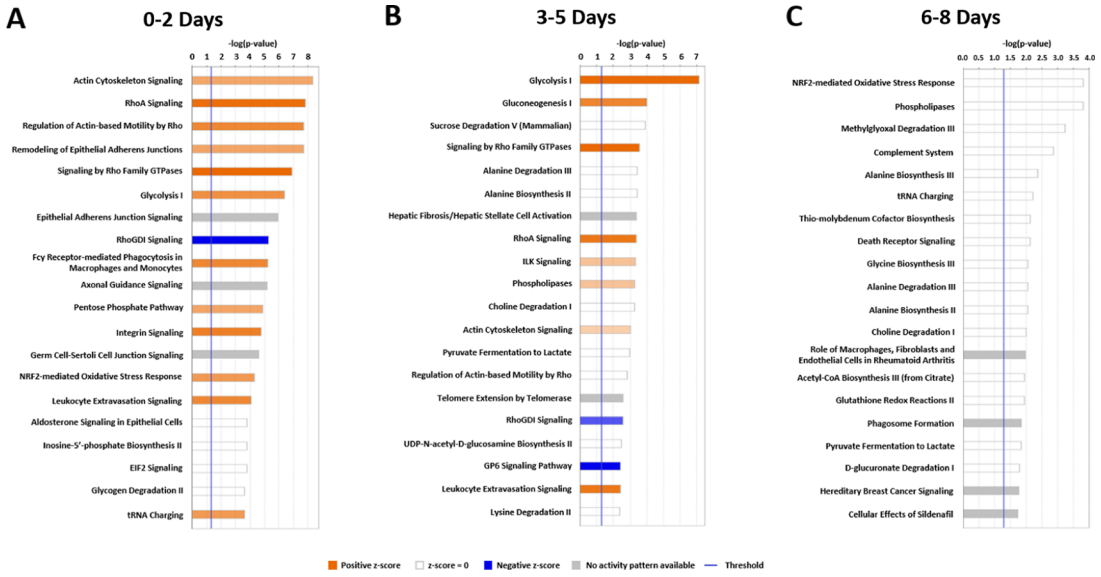

Figure 7. Altered canonical pathways associated with differentially abundant metabolites and proteins within the culture media at (A) 0–2 days, (B) 3–5 days, and (C) 6–8 days following TNF-α/IL-1β treatment of *ex vivo* equine cartilage explants. Canonical pathway significance was calculated using a right-sided Fisher's exact test and represented by the associated bars. The highest values represent canonical pathways, which are least likely to have been identified due to random chance. Blue represents downregulated canonical pathways and orange represents upregulated canonical pathways.

1β treatment. Additionally, a protein band of molecular weight 160–260 kDa was identified as reduced in the treated media compared to that in control samples *via* 1D SDS PAGE, which may be representing fibronectin (250 kDa), although further techniques, *i.e.*, western blotting or MS/MS analysis of an in-gel tryptic digest, are required to confirm this.[69,70] However, elevated levels of fibronectin have previously been identified within OA SF, with fibronectin found to localize at sites of cartilage degeneration and subsequently secreted into the ECM by equine chondrocytes.[71,72] The reasons for this possible discrepancy in results between this study and previous studies are currently not known and require further investigation. It may be that within this study fibronectin has undergone post-translational modifications following treatment, which may not have been identified *via* the PEAKS identification algorithm or resulted in ions that subsequently did not "fly" well during MS analysis and thus were subsequently not identified as peptides.

Our study benefited by the integrated pathway analysis of metabolites and proteins. Pathways implicated within this study were dominated by the upregulation of cellular movement pathways, particularly within the earlier stages of the OA model, including actin cytoskeleton signaling, signaling by Rho GTPases, and RhoA signaling. The actin cytoskeleton is known to be regulated by Rho GTPase upstream regulators, with RhoA having been identified as having an important role in the regulation of cytoskeletal structure and focal adhesion maturation.[73,74] The RhoA/ROCK (Rho-associated kinase) pathway has previously been established as having a critical function within the regulation of chondrocyte proliferation and differentiation, suppressing chondrogenesis by decreasing the expression of the chondrocyte transcription factor Sox9.[74,75] Targeting this pathway may therefore provide a critical role in the development of cartilage tissue constructs, which are clinically translatable, to treat OA.[76] Additionally, with an increasing body of evidence implicating the RhoA/ROCK pathway within OA development, this pathway is currently being investigated as a potentially novel therapeutic target within the patient's own cartilage.[77] Therefore, with activation of these pathways identified within this *ex vivo* cartilage model of early OA, interrogating combined changes in the metabolome and proteome within this model may have a

https://dx.doi.org/10.1021/acs.jproteome.0c00143
J. Proteome Res. 2020, 19, 3652–3667

beneficial role in testing responses of novel therapeutics on the actin cytoskeleton/Rho GTPase pathways.

Following TNF-α/IL-1β treatment, elevations of glucose within the cartilage were identified. This is supported by a previous study, which demonstrated that TNF-α and IL-1β upregulate glucose transport in chondrocytes through the upregulation of glucose transporter (GLUT)1 and GLUT9 mRNA synthesis with increased levels of glycosylated GLUT1 incorporated into the plasma membrane.[78] This influx in glucose is likely, at least in part, to be due to the increased energy requirement following cytokine stimulation in the production of MMPs and secretion of IL-6, IL-8, hematopoietic colony-stimulating factor, and prostaglandin E_2.[79] In addition, although glucose was not identified within the culture media, glycolysis and gluconeogenesis pathways were predicted to be upregulated based on numerous differentially abundant proteins within these pathways, including enolase 1. Enolase 1 is a multifunctional glycolytic enzyme, which has previously been shown to have increased abundance within an equine articular cartilage model stimulated with IL-1β, as well as increased expression on the cell surface of immune cells during rheumatoid arthritis (RA).[70,80] Lee et al. identified apolipoprotein B within RA SF to be a specific ligand to enolase 1, provoking an inflammatory response. Elevated levels of apolipoprotein B have also been associated with human knee OA.[81] Thus, lipid metabolism may operate through this mechanism to regulate chronic inflammation in OA, as well as RA.[80]

Within gluconeogenesis, the 10 differentially abundant molecules identified within this pathway also included enolase 1, as well as alanine and choline. Across the whole study, alanine was found to be a central component in discriminating control and treatment groups. Alanine levels were depleted in treated cartilage extracts compared to those in controls and were identified as an important component in discriminating control and treated cartilage samples. Reduced alanine levels were also identified in human OA cartilage using HRMAS NMR spectroscopy.[52] Within the culture media, alanine was depleted at all time points in the treated samples, and involvement of alanine degradation and biosynthesis pathways was identified as significant. Alanine has previously been identified as a key component of the metabolic urinary OA profile of guinea pigs.[82] A ^{1}H NMR metabolomics study of equine SF also identified elevated levels of choline in OA.[43] However, elevated levels of alanine and citrate were also identified, while these were found to be decreased within our study.

Upregulation of molecular transport pathways was driven by numerous differentially expressed metabolites and proteins, including alanine, citrate, arginine, choline, RhoC, COMP, and MMP-3. Along with actin cytoskeleton regulation, Rho GTPases are also known to regulate vesicle movement through vesicle trafficking, with ROCK1 colocalizing with vesicles and involved in microvesicle production.[74,83,84] Extracellular vesicles are now known to play an important role within OA pathogenesis, with their structure and cargo being a growing area within OA research.[85,86] It would therefore be of interest to use the techniques used within this study to interrogate the metabolite and protein cargo of extracellular vesicles within this early OA model.

Within this study, arginine levels were initially identified as decreased following treatment at the earliest time point. A recent study of human plasma also identified arginine to be depleted in knee OA.[87] The authors proposed that this is due to increased activity of the conversion of arginine to ornithine resulting in an imbalance between cartilage repair and degradation. This is supported by a recent learning and network approach of OA-associated metabolites, in which arginine and ornithine appeared in about 30 and 25% of the generated models studied, respectively.[88] In addition to this, a reduction in arginine may be reflective of an increased production of nitric oxide (L-arginine being converted to NOH-arginine and subsequently L-citrulline and nitric oxide), as identified in the human OA cartilage.[89,90]

The cytoplasm organization pathway was identified as significantly altered at 0−2 days, driven partially by reduced alanine levels and increased levels of RhoC and vimentin. Vimentin is a multifunctional intermediate filament protein.[91] Within chondrocytes, it has been demonstrated that vimentin is likely to be involved in mechanotransduction.[92] Our results are supported by a previous study, which identified elevated levels of cleaved vimentin within the human OA cartilage, with distortion of the vimentin network evident.[93]

Isoleucine was elevated within the media during the latter stages of the model. Elevated isoleucine levels have previously been reported within the SF of a canine OA model and human OA serum.[41,94] Borel et al. previously identified elevations of peaks within ^{1}H HRMAS NMR spectra of OA cartilage, which could be attributed to isoleucine.[51] Thus, the elevations seen in isoleucine may be reflective of a cartilage collagen breakdown.[94] However, within this study, although a higher abundance was recorded for isoleucine in treated compared to that in control cartilage, this did not reach statistical significance. Furthermore, elevations in glutamate were identified within the culture media at 3−5 days, consistent with a previous study, which may be resultant of the catabolism of collagenous proline through proline oxidase.[27,95] Reduced levels of collagen type VI α 2 chain and collagen type X α 1 chain were identified at 3−5 and 6−8 days following cytokine treatment. This may reflect a reduction in collagen synthesis, which has previously been identified within other collagen types following TNF-α/IL-1β stimulation.[22] Therefore, these results provide evidence of a disruption in collagen homeostasis and suggest that collagens are being degraded within the model sooner than the 14−28 days previously reported within other *ex vivo* cartilage OA models.[96,97]

Coagulation factor XIII A chain, fibromodulin, and lamin A/C levels were all identified as being elevated within culture media following TNF-α/IL-1β treatment at the earliest time point: 0−2 days. All three of these proteins were also identified as involved in alterations to cellular movement pathways, which have been central to the biological changes within the earlier stages of this OA model.

Coagulation factor XIII is a heterotetrameric protein complex, which cross-links fibrin polymers through covalent bonds.[98] Coagulation factor XIII A chain immunostaining was previously found to be elevated within human articular knee cartilage following IL-1β stimulation.[99] Sanchez et al. identified increased expression of coagulation factor XIII A chain in osteoblasts within the sclerotic zone of the OA subchondral bone.[100] Clinically, remodeling of the subchondral bone is likely to be closely related to cartilage degradation.[101] Within hypertrophic chondrocytes, Nurminskaya et al. concluded that cell death and lysis were responsible for the externalization of the protein.[102] However, coagulation factor XIII A chain has also been identified within articular cartilage vesicles, although

https://dx.doi.org/10.1021/acs.jproteome.0c00143
J. Proteome Res. 2020, 19, 3652−3667

the underlying externalization mechanism remains unknown.[103]

Fibromodulin is a small leucine-rich repeat proteoglycan that interacts with collagen fibrils and influences fibrillogenesis rate and fibril structure.[104] Experimental mice, which lack biglycan and fibromodulin, have been shown to develop OA in multiple joints.[105,106] Neopeptides generated from fibromodulin degradation have also been identified as potential markers of equine articular cartilage degradation.[30]

Within our study, higher levels of lamin A/C (intermediate filament protein) were identified within the treated media samples.[107] Lamin A/C has also been identified as being upregulated in human OA cartilage, and elevated levels have been implicated in the dysregulation of chondrocyte autophagy in aging and OA.[108,109] Thus, our results support these studies, with chondrocyte autophagy targeting a potential novel therapeutic route.

Due to an elevation in enzymatic activity and breakdown of cartilage during OA, potential biomarkers include ECM degradation fragments.[110] PCA identified that the semitryptic peptide profiles generated from the treated equine cartilage were less variable than those of the controls, demonstrating that the TNF-α/IL-1β treatment is driving the semitryptic peptide profile within the model. Within this study, we have identified several semitryptic peptides (potential neopeptides) that were identified as being elevated following treatment compared to those of controls, including degradation products from the ECM proteins aggrecan, cartilage intermediate layer protein, vimentin, and collagen type VI. None of these potential neopeptides have previously been identified within the literature.[30,35,36,70]

Study Limitations

Previously, an *in vivo* study of equine OA identified physiological levels of TNF-α and IL-1β within SF to be 40−80 pg/mL.[19] However, our study, along with previous studies in the field, has used significantly higher cytokine concentrations to experimentally model OA.[20−25,27,28] This approach was used within this study due to the short half-lives of these two cytokines.[111,112] Supplementation at a concentration closer to the physiological levels would have ultimately resulted in the experiment being largely conducted with cytokine levels significantly below that experienced during OA, thus producing results that may have been of insufficient benefit. Therefore, the approach used within this study to model OA should be taken into consideration when interpreting the results.

The cytokine preparations used within this study contained various metabolites, which, following their removal from subsequent statistical analysis, prevented the analysis of some various metabolites within the experiment. Additionally, the culture media was supplemented with a protease inhibitor cocktail at collection to inhibit the general protein degradation prior to MS proteomic analysis, with results therefore representing the peptide/protein composition during experimentation. However, the high mannitol content prevented analysis of this metabolite within the sample/spectral region. Therefore, when in future, using cytokines/supplements for NMR metabolomics, analyzing the spectra of different manufacturers/preparations prior to experimentation may be beneficial to identify their associated metabolite profiles, selecting the most appropriate products to maximize the downstream interpretation of results.

Further Work

Within this study, OA was modeled using a combined treatment of TNF-α and IL-1β. Now that this paper has optimized a method to extract metabolites from the articular cartilage for ^{1}H NMR analysis and protocols established to concurrently investigate metabolite and protein profiles within culture media, it may be of interest to subsequently explore the effect of individual cytokine treatments, separate TNF-α and IL-1β treatments, comparing these results to those identified within this study. Additional MS-based metabolomics analysis of the culture media within this study may be beneficial as NMR and MS are complementary techniques and would therefore expand the number of identified/quantified metabolites, additionally identifying potential lipid and carbohydrate profiles of interest.[9,40,45,113] To confirm the differentially abundant proteins within this study, validation using an orthologous technique, *e.g.*, Western blotting or enzyme-linked immunosorbent assays, is required. Further validation of potential neopeptides could also be carried out through multiple reaction monitoring using a triple-quadrupole mass spectrometer.[114] Following this, the development of monoclonal antibodies specific to neopeptides of interest would enable simpler monitoring of neopeptide abundance in *in vitro*, *ex vivo*, and clinical environments.[115] Following validations, monitoring the differentially abundant metabolites, proteins, and neopeptides within this study within longitudinal SF samples from OA horses would identify the translation of these findings to a clinical setting and the eventual generation of clinically applicable diagnostic tests.

CONCLUSIONS

In conclusion, this is the first study to use a multi-"omics" approach to simultaneously investigate the metabolomic profile of *ex vivo* cartilage and metabolomic/proteomic profiles of culture media using the TNF-α/IL-1β *ex vivo* OA cartilage model. We have identified a panel of metabolites and proteins that are differentially abundant within an early phase of the OA model, 0−2 days, which may provide further information on the underlying disease pathogenesis, as well as the potential to translate to clinical markers. Altered pathways implicated within this model were largely dominated by those involved in cellular movement. This study has also identified a panel of ECM-derived neopeptides that have the potential to help enable OA stratification, as well as provide potential novel therapeutic targets.

ASSOCIATED CONTENT

Supporting Information

The Supporting Information is available free of charge at https://pubs.acs.org/doi/10.1021/acs.jproteome.0c00143.

Liquid chromatography-tandem mass spectrometry—detailed methods; five postmortem equine metacarpophalangeal joints used for *ex vivo* cartilage culture (Figure S1); experimental design for *ex vivo* equine cartilage culture ± TNF-α/IL-1β treatment (Figure S2); 1D ^{1}H nuclear magnetic resonance spectral quantile plots of cartilage, 8 days in control media; cartilage, 8 days in TNF-α/IL-1β-treated media; control media (all time points combined); and TNF-α/IL-1β-treated media (all time points combined) (Figure S3); representative culture media ion chromatograms of combined time points for control and TNF-α/IL-1β-

https://dx.doi.org/10.1021/acs.jproteome.0c00143
J. Proteome Res. 2020, 19, 3652−3667

treated equine *ex vivo* cartilage explants using a 60 min liquid chromatography gradient (Figure S4); principal component analysis score plot identifying high reproducibility of acetonitrile cartilage metabolite extraction (three separate equine donors, technical triplicate for each donor) using 1D ^{1}H NMR metabolome analysis (Figure S5); PC1 RMS values for the 25 components with the highest magnitude for differentially abundant proteins present within culture media at (A) 0−2 days, (B) 3−5 days, and (C) 6−8 days following TNF-α/IL-1β treatment of *ex vivo* equine cartilage (Figure S6); silver stain-identifying media protein profiles (combined for all time points) following incubation of *ex vivo* equine cartilage for control and TNF-α/IL-1β-treated samples (Figure S7); principal component analyses of semitryptic peptide profiles within the culture media of control and TNF-α/IL-1β-treated *ex vivo* equine cartilage at 0−2, 3−5, and 6−8 days (Figure S8); heat maps identifying canonical pathway groupings associated with diseases and biological functions altered for 0−2, 3−5, and 6−8 days within culture media following TNF-α/IL-1β treatment of *ex vivo* equine cartilage explants (Figure S9); networks involved in cell movement, migration of cells, and invasion of cells in culture media at 0−2 days following TNF-α/IL-1β treatment of *ex vivo* equine cartilage explants (Figure S10); all proteins identified within culture media, including control and TNF-α/IL-1β-treated *ex vivo* equine cartilage sample wells (Table S1) (PDF)

AUTHOR INFORMATION

Corresponding Author

James R. Anderson − *Musculoskeletal and Ageing Science, Institute of Life Course and Medical Sciences, University of Liverpool, Liverpool L7 8TX, U.K.;* orcid.org/0000-0003-0489-7997; Phone: 01517949287; Email: janders@liverpool.ac.uk

Authors

Marie M. Phelan − *NMR Metabolomics Facility, Technology Directorate & Department of Biochemistry & Systems Biology, Institute of Systems, Molecular and Integrative Biology, University of Liverpool, Liverpool L69 7ZB, U.K.*

Laura Foddy − *School of Veterinary Science, Institute of Infection, Veterinary & Ecological Sciences, University of Liverpool, Liverpool L69 3GH, U.K.*

Peter D. Clegg − *Musculoskeletal and Ageing Science, Institute of Life Course and Medical Sciences, University of Liverpool, Liverpool L7 8TX, U.K.*

Mandy J. Peffers − *Musculoskeletal and Ageing Science, Institute of Life Course and Medical Sciences, University of Liverpool, Liverpool L7 8TX, U.K.;* orcid.org/0000-0001-6979-0440

Complete contact information is available at: https://pubs.acs.org/10.1021/acs.jproteome.0c00143

Author Contributions

J.R.A. wrote the manuscript; J.R.A., M.M.P., P.D.C., and M.J.P. revised the manuscript; J.R.A. collected cartilage samples; J.R.A., L.F., and M.M.P. carried out experimental procedures and analyzed the data; and J.R.A., M.M.P., P.D.C., and M.J.P. carried out experimental design. All authors read and approved the final manuscript.

Funding

J.R.A. was funded through a Horse Trust Ph.D. studentship (G1015) and M.J.P. was funded through a Wellcome Trust Intermediate Clinical Fellowship (107471/Z/15/Z). Software licenses for data analysis used in the Shared Research Facility for NMR metabolomics were funded by the Medical Research Council (MRC) Clinical Research Capabilities and Technologies Initiative (MR/M009114/1). This work was also supported by the MRC and Versus Arthritis as part of the Medical Research Council Versus Arthritis Centre for Integrated Research into Musculoskeletal Ageing (CIMA) [MR/R502182/1]. The MRC Versus Arthritis Centre for Integrated Research into Musculoskeletal Ageing is a collaboration between the Universities of Liverpool, Sheffield, and Newcastle.

Notes

The authors declare no competing financial interest.

Cartilage samples were collected as a byproduct of the agricultural industry. The Animals (Scientific Procedures) Act 1986, Schedule 2, does not define collection from these sources as scientific procedures, and ethical approval was therefore not required.

ACKNOWLEDGMENTS

The authors would like to thank the staff at F Drury and Sons, Abattoir, Swindon, for their assistance in sample collection; the members of the Centre for Protein Research, University of Liverpool, including Prof. Rob Beynon and Dr. Philip Brownridge, for mass spectrometry access and advice; Dr. Olivia Alder, Qiagen, for Ingenuity Pathway Analysis support; and Jake Ellis, Cardiff University, for undertaking NMR file depositions.

ABBREVIATIONS

ADAMTS, a disintegrin and metalloproteinase with thrombospondin motifs; CPMG, Carr−Purcell−Meiboom−Gill; COMP, cartilage oligomeric matrix protein; DMEM, Dulbecco's modified Eagle's medium; EDTA, ethylenediaminetetraacetic acid; ECM, extracellular matrix; FDR, false discovery rate; FCS, fetal calf serum; GLUT, glucose transporter; HRMAS, high-resolution magical angle spinning; IL-1β, interleukin-1β; MS, mass spectrometry; MMP, matrix metalloproteinase; MSI, metabolomics Standards Initiative; NMR, nuclear magnetic resonance; 1D SDS PAGE, one-dimensional sodium dodecyl sulfate polyacrylamide gel electrophoresis; OA, osteoarthritis; PBS, phosphate-buffered saline; PCA, principal component analysis; PC1, principal component 1; PQN, probabilistic quotient normalization; RA, rheumatoid arthritis; Rho, Ras homologue gene family; RMS, root mean square; ROCK, Rho-associated kinase; SF, synovial fluid; TIC, total ion current; TFA, trifluoroacetic acid; TSP, trimethylsilyl propionate; TNF-α, tumor necrosis factor-α

REFERENCES

(1) Truong, L.-H.; Kuliwaba, J. S.; Tsangari, H.; Fazzalari, N. L. Differential Gene Expression of Bone Anabolic Factors and Trabecular Bone Architectural Changes in the Proximal Femoral Shaft of Primary Hip Osteoarthritis Patients. *Arthritis Res. Ther.* **2006**, *8*, R188.

(2) Kramer, C. M.; Tsang, A. S.; Koenig, T.; Jeffcott, L. B.; Dart, C. M.; Dart, A. J. Survey of the Therapeutic Approach and Efficacy of Pentosan Polysulfate for the Prevention and Treatment of Equine

Osteoarthritis in Veterinary Practice in Australia. *Aust. Vet. J.* **2014**, *92*, 482−487.
(3) Ireland, J. L.; Clegg, P. D.; McGowan, C. M.; Platt, L.; Pinchbeck, G. L. Factors Associated with Mortality of Geriatric Horses in the United Kingdom. *Prev. Vet. Med.* **2011**, *101*, 204−218.
(4) Ireland, J. L.; Clegg, P. D.; McGowan, C. M.; McKane, S. A.; Chandler, K. J.; Pinchbeck, G. L. Disease Prevalence in Geriatric Horses in the United Kingdom: Veterinary Clinical Assessment of 200 Cases. *Equine Vet. J.* **2012**, *44*, 101−106.
(5) Caron, J.; Genovese, R. Principles and Practices of Joint Disease Treatment. In *Diagnosis and Management of Lameness in the Horse*; Ross, M.; Dyson, S., Eds.; W.B. Saunders: Philadelphia, 2003; pp 746−764.
(6) Struglics, A.; Larsson, S.; Pratta, M. A.; Kumar, S.; Lark, M. W.; Lohmander, L. S. Human Osteoarthritis Synovial Fluid and Joint Cartilage Contain Both Aggrecanase- and Matrix Metalloproteinase-Generated Aggrecan Fragments. *Osteoarthritis Cartilage* **2006**, *14*, 101−113.
(7) Li, Y.; Xu, L.; Olsen, B. R. Lessons from Genetic Forms of Osteoarthritis for the Pathogenesis of the Disease. *Osteoarthritis Cartilage* **2007**, *15*, 1101−1105.
(8) Marhardt, K.; Muurahainen, N. Development of a Disease-Modifying OA Drug (DMOAD) in Knee Osteoarthritis: The Example of Sprifermin. *Drug Res.* **2015**, *65*, S13.
(9) Anderson, J. R.; Phelan, M. M.; Clegg, P. D.; Peffers, M. J.; Rubio-Martinez, L. M. Synovial Fluid Metabolites Differentiate between Septic and Nonseptic Joint Pathologies. *J. Proteome Res.* **2018**, *17*, 2735−2743.
(10) Brommer, H.; van Weeren, P. R.; Brama, P. A. New Approach for Quantitative Assessment of Articular Cartilage Degeneration in Horses with Osteoarthritis. *Am. J. Vet. Res.* **2003**, *64*, 83−87.
(11) Hunter, D. J.; Nevitt, M.; Losina, E.; Kraus, V. Biomarkers for Osteoarthritis: Current Position and Steps towards Further Validation. *Best Pract. Res. Clin. Rheumatol.* **2014**, *28*, 61−71.
(12) McIlwraith, C. W.; Kawcak, C. E.; Frisbie, D. D.; Little, C. B.; Clegg, P. D.; Peffers, M. J.; Karsdal, M. A.; Ekman, S.; Laverty, S.; Slayden, R. A.; et al. Biomarkers for Equine Joint Injury and Osteoarthritis. *J. Orthop. Res.* **2018**, *36*, 823−831.
(13) Wojdasiewicz, P.; Poniatowski, Ł. A.; Szukiewicz, D. The Role of Inflammatory and Anti-Inflammatory Cytokines in the Pathogenesis of Osteoarthritis. *Mediators Inflamm.* **2014**, *2014*, No. 561459.
(14) Wang, J.; Markova, D.; Anderson, D. G.; Zheng, Z.; Shapiro, I. M.; Risbud, M. V. TNF-α and IL-1β Promote a Disintegrin-like and Metalloprotease with Thrombospondin Type I Motif-5-Mediated Aggrecan Degradation through Syndecan-4 in Intervertebral Disc. *J. Biol. Chem.* **2011**, *286*, 39738−39749.
(15) Fernandes, J. C.; Martel-Pelletier, J.; Pelletier, J.-P. The Role of Cytokines in Osteoarthritis Pathophysiology. *Biorheology* **2002**, *39*, 237−246.
(16) Goldring, S. R.; Goldring, M. B. The Role of Cytokines in Cartilage Matrix Degeneration in Osteoarthritis. *Clin. Orthop. Relat. Res.* **2004**, *427*, S27−S36.
(17) Westacott, C. I.; Whicher, J. T.; Barnes, I. C.; Thompson, D.; Swan, A. J.; Dieppe, P. A. Synovial Fluid Concentration of Five Different Cytokines in Rheumatic Diseases. *Ann. Rheum. Dis.* **1990**, *49*, 676−681.
(18) Bertuglia, A.; Pagliara, E.; Grego, E.; Ricci, A.; Brkljaca-Bottegaro, N. Pro-Inflammatory Cytokines and Structural Biomarkers Are Effective to Categorize Osteoarthritis Phenotype and Progression in Standardbred Racehorses over Five Years of Racing Career. *BMC Vet. Res.* **2016**, *12*, No. 246.
(19) Ma, T.-W.; Li, Y.; Wang, G.-Y.; Li, X.-R.; Jiang, R.-L.; Song, X.-P.; Zhang, Z.-H.; Bai, H.; Li, X.; Gao, L. Changes in Synovial Fluid Biomarkers after Experimental Equine Osteoarthritis. *J. Vet. Res.* **2017**, *61*, 503−508.
(20) Williams, A. Proteomic Studies of an Explant Model of Equine Articular Cartilage in Response to Proinflammatory and Anti-Inflammatory Stimuli, Ph.D. Thesis, University of Nottingham, 2014.
(21) Stevens, A. L.; Wishnok, J. S.; Chai, D. H.; Grodzinsky, A. J.; Tannenbaum, S. R. A Sodium Dodecyl Sulfate-Polyacrylamide Gel Electrophoresis-Liquid Chromatography Tandem Mass Spectrometry Analysis of Bovine Cartilage Tissue Response to Mechanical Compression Injury and the Inflammatory Cytokines Tumor Necrosis Factor α and Interleukin-1β. *Arthritis Rheum.* **2008**, *58*, 489−500.
(22) Stevens, A. L.; Wishnok, J. S.; White, F. M.; Grodzinsky, A. J.; Tannenbaum, S. R. Mechanical Injury and Cytokines Cause Loss of Cartilage Integrity and Upregulate Proteins Associated with Catabolism, Immunity, Inflammation, and Repair. *Mol. Cell. Proteomics* **2009**, *8*, 1475−1489.
(23) Pretzel, D.; Pohlers, D.; Weinert, S.; Kinne, R. W. In Vitro Model for the Analysis of Synovial Fibroblast-Mediated Degradation of Intact Cartilage. *Arthritis Res. Ther.* **2009**, *11*, No. R25.
(24) De Ceuninck, F.; Dassencourt, L.; Anract, P. The Inflammatory Side of Human Chondrocytes Unveiled by Antibody Microarrays. *Biochem. Biophys. Res. Commun.* **2004**, *323*, 960−969.
(25) Cillero-Pastor, B.; Ruiz-Romero, C.; Caramés, B.; López-Armada, M. J.; Blanco, F. J. Proteomic Analysis by Two-Dimensional Electrophoresis to Identify the Normal Human Chondrocyte Proteome Stimulated by Tumor Necrosis Factor α and Interleukin-1β. *Arthritis Rheum.* **2010**, *62*, 802−814.
(26) Barksby, H. E.; Milner, J. M.; Patterson, A. M.; Peake, N. J.; Hui, W.; Robson, T.; Lakey, R.; Middleton, J.; Cawston, T. E.; Richards, C. D.; et al. Matrix Metalloproteinase 10 Promotion of Collagenolysis via Procollagenase Activation: Implications for Cartilage Degradation in Arthritis. *Arthritis Rheum.* **2006**, *54*, 3244−3253.
(27) Fellows, C.; Quasnichka, H.; Chowdhury, N. R.; Budd, E.; Skene, D. J.; Mobasheri, A.; Overmyer, K. A.; Muir, P.; Coon, J. J.; Cheleschi, S.; et al. Metabolomics and Metabolic Function Analysis of the Secretome of Articular Cartilage and Isolated Chondrocytes in Response to Pro-Inflammatory Cytokines. *Osteoarthritis Cartilage* **2018**, *26*, S172.
(28) Jeremiasse, B.; Matta, C.; Fellows, C. R.; Boocock, D. J.; Smith, J. R.; Liddell, S.; Lafeber, F.; van Spil, W. E.; Mobasheri, A. Alterations in the Chondrocyte Surfaceome in Response to Pro-Inflammatory Cytokines. *BMC Mol. Cell Biol.* **2020**, *21*, No. 47.
(29) de Hoog, C. L.; Mann, M. Proteomics. *Annu. Rev. Genomics Hum. Genet.* **2004**, *5*, 267−293.
(30) Peffers, M. J.; Thornton, D. J.; Clegg, P. D. Characterization of Neopeptides in Equine Articular Cartilage Degradation. *J. Orthop. Res.* **2016**, *34*, 106−120.
(31) Polur, I.; Lee, P. L.; Servais, J. M.; Xu, L.; Li, Y. Role of HTRA1, a Serine Protease, in the Progression of Articular Cartilage Degeneration. *Histol. Histopathol.* **2010**, *25*, 599−608.
(32) Ben-Aderet, L.; Merquiol, E.; Fahham, D.; Kumar, A.; Reich, E.; Ben-Nun, Y.; Kandel, L.; Haze, A.; Liebergall, M.; Kosińska, M. K.; et al. Detecting Cathepsin Activity in Human Osteoarthritis via Activity-Based Probes. *Arthritis Res. Ther.* **2015**, *17*, No. 69.
(33) Peffers, M. J.; Smagul, A.; Anderson, J. R. Proteomic Analysis of Synovial Fluid: Current and Potential Uses to Improve Clinical Outcomes. *Expert Rev. Proteomics* **2019**, *16*, 287−302.
(34) Miller, R. E.; Ishihara, S.; Tran, P. B.; Golub, S. B.; Last, K.; Miller, R. J.; Fosang, A. J.; Malfait, A.-M. An Aggrecan Fragment Drives Osteoarthritis Pain through Toll-like Receptor 2. *JCI Insight* **2018**, *3*, No. e95704.
(35) Peffers, M. J.; Cillero-Pastor, B.; Eijkel, G. B.; Clegg, P. D.; Heeren, R. M. Matrix Assisted Laser Desorption Ionization Mass Spectrometry Imaging Identifies Markers of Ageing and Osteoarthritic Cartilage. *Arthritis Res. Ther.* **2014**, *16*, No. R110.
(36) Peffers, M. J.; McDermott, B.; Clegg, P. D.; Riggs, C. M. Comprehensive Protein Profiling of Synovial Fluid in Osteoarthritis Following Protein Equalization. *Osteoarthritis Cartilage* **2015**, *23*, 1204−1213.
(37) Skiöldebrand, E.; Ekman, S.; Mattsson Hultén, L.; Svala, E.; Björkman, K.; Lindahl, A.; Lundqvist, A.; Önnerfjord, P.; Sihlbom, C.; Rüetschi, U. Cartilage Oligomeric Matrix Protein Neoepitope in the

https://dx.doi.org/10.1021/acs.jproteome.0c00143
J. Proteome Res. 2020, 19, 3652−3667

Synovial Fluid of Horses with Acute Lameness: A New Biomarker for the Early Stages of Osteoarthritis. *Equine Vet. J.* **2017**, *49*, 662−667.
(38) Peffers, M.; Jones, A. R.; McCabe, A.; Anderson, J. Neopeptide Analyser: A Software Tool for Neopeptide Discovery in Proteomics Data. *Wellcome Open Res.* **2017**, *2*, 24.
(39) Beckonert, O.; Keun, H. C.; Ebbels, T. M. D.; Bundy, J.; Holmes, E.; Lindon, J. C.; Nicholson, J. K. Metabolic Profiling, Metabolomic and Metabonomic Procedures for NMR Spectroscopy of Urine, Plasma, Serum and Tissue Extracts. *Nat. Protoc.* **2007**, *2*, 2692−2703.
(40) Beltran, A.; Suarez, M.; Rodríguez, M. A.; Vinaixa, M.; Samino, S.; Arola, L.; Correig, X.; Yanes, O. Assessment of Compatibility between Extraction Methods for NMR- and LC/MS-Based Metabolomics. *Anal. Chem.* **2012**, *84*, 5838−5844.
(41) Damyanovich, A. Z.; Staples, J. R.; Chan, A. D.; Marshall, K. W. Comparative Study of Normal and Osteoarthritic Canine Synovial Fluid Using 500 MHz 1H Magnetic Resonance Spectroscopy. *J. Orthop. Res.* **1999**, *17*, 223−231.
(42) Hugle, T.; Kovacs, H.; Heijnen, I. A.; Daikeler, T.; Baisch, U.; Hicks, J. M.; Valderrabano, V. Synovial Fluid Metabolomics in Different Forms of Arthritis Assessed by Nuclear Magnetic Resonance Spectroscopy. *Clin. Exp. Rheumatol.* **2012**, *30*, 240−245.
(43) Lacitignola, L.; Fanizzi, F. P.; Francioso, E.; Crovace, A. 1H NMR Investigation of Normal and Osteo-Arthritic Synovial Fluid in the Horse. *Vet. Comp. Orthop. Traumatol.* **2008**, *21*, 85−88.
(44) Mickiewicz, B.; Heard, B. J.; Chau, J. K.; Chung, M.; Hart, D. A.; Shrive, N. G.; Frank, C. B.; Vogel, H. J. Metabolic Profiling of Synovial Fluid in a Unilateral Ovine Model of Anterior Cruciate Ligament Reconstruction of the Knee Suggests Biomarkers for Early Osteoarthritis. *J. Orthop. Res.* **2015**, *33*, 71−77.
(45) Mickiewicz, B.; Kelly, J. J.; Ludwig, T. E.; Weljie, A. M.; Wiley, J. P.; Schmidt, T. A.; Vogel, H. J. Metabolic Analysis of Knee Synovial Fluid as a Potential Diagnostic Approach for Osteoarthritis. *J. Orthop. Res.* **2015**, *33*, 1631−1638.
(46) Anderson, J. R.; Chokesuwattanaskul, S.; Phelan, M. M.; Welting, T. J. M.; Lian, L.-Y.; Peffers, M. J.; Wright, H. L. 1H NMR Metabolomics Identifies Underlying Inflammatory Pathology in Osteoarthritis and Rheumatoid Arthritis Synovial Joints. *J. Proteome Res.* **2018**, *17*, 3780−3790.
(47) Graham, R. J. T. Y.; Anderson, J. R.; Phelan, M. M.; Cillan-Garcia, E.; Bladon, B. M.; Taylor, S. E. Metabolomic Analysis of Synovial Fluid from Thoroughbred Racehorses Diagnosed with Palmar Osteochondral Disease Using Magnetic Resonance Imaging. *Equine Vet. J.* **2020**, *52*, 384−390.
(48) Ling, W.; Regatte, R. R.; Schweitzer, M. E.; Jerschow, A. Characterization of Bovine Patellar Cartilage by NMR. *NMR Biomed.* **2008**, *21*, 289−295.
(49) Schiller, J.; Huster, D.; Fuchs, B.; Naji, L.; Kaufmann, J.; Arnold, K. Evaluation of Cartilage Composition and Degradation by High-Resolution Magic-Angle Spinning Nuclear Magnetic Resonance. *Cartilage Osteoarthritis*; Humana Press: New Jersey, 2004; pp 267−286.
(50) Schiller, J.; Naji, L.; Huster, D.; Kaufmann, J.; Arnold, K. 1H and 13C HR-MAS NMR Investigations on Native and Enzymatically Digested Bovine Nasal Cartilage. *MAGMA* **2001**, *13*, 19−27.
(51) Borel, M.; Pastoureau, P.; Papon, J.; Madelmont, J. C.; Moins, N.; Maublant, J.; Miot-Noirault, E. Longitudinal Profiling of Articular Cartilage Degradation in Osteoarthritis by High-Resolution Magic Angle Spinning ^{1}H NMR Spectroscopy: Experimental Study in the Meniscectomized Guinea Pig Model. *J. Proteome Res.* **2009**, *8*, 2594−2600.
(52) Shet, K.; Siddiqui, S. M.; Yoshihara, H.; Kurhanewicz, J.; Ries, M.; Li, X. High-Resolution Magic Angle Spinning NMR Spectroscopy of Human Osteoarthritic Cartilage. *NMR Biomed.* **2012**, *25*, 538−544.
(53) McIlwraith, C. W.; Frisbie, D. D.; Kawcak, C. E.; Fuller, C. J.; Hurtig, M.; Cruz, A. The OARSI Histopathology Initiative − Recommendations for Histological Assessments of Osteoarthritis in the Horse. *Osteoarthritis Cartilage* **2010**, *18*, S93−S105.
(54) Sumner, L. W.; Amberg, A.; Barrett, D.; Beale, M. H.; Beger, R.; Daykin, C. A.; Fan, T. W.; Fiehn, O.; Goodacre, R.; Griffin, J. L.; et al. Proposed Minimum Reporting Standards for Chemical Analysis Chemical Analysis Working Group (CAWG) Metabolomics Standards Initiative (MSI). *Metabolomics* **2007**, *3*, 211−221.
(55) Haug, K.; Cochrane, K.; Nainala, V. C.; Williams, M.; Chang, J.; Jayaseelan, K. V.; O'Donovan, C. MetaboLights: A Resource Evolving in Response to the Needs of Its Scientific Community. *Nucleic Acids Res.* **2019**, *48*, D440.
(56) Perez-Riverol, Y.; Csordas, A.; Bai, J.; Bernal-Llinares, M.; Hewapathirana, S.; Kundu, D. J.; Inuganti, A.; Griss, J.; Mayer, G.; Eisenacher, M.; et al. The PRIDE Database and Related Tools and Resources in 2019: Improving Support for Quantification Data. *Nucleic Acids Res.* **2019**, *47*, D442−D450.
(57) Dieterle, F.; Ross, A.; Schlotterbeck, G.; Senn, H. Probabilistic Quotient Normalization as Robust Method to Account for Dilution of Complex Biological Mixtures. Application in 1H NMR Metabonomics. *Anal. Chem.* **2006**, *78*, 4281−4290.
(58) Worley, B.; Powers, R. Multivariate Analysis in Metabolomics. *Curr. Metabolomics* **2013**, *1*, 92−107.
(59) Benjamini, Y.; Hochberg, Y. Controlling the False Discovery Rate: A Practical and Powerful Approach to Multiple Testing. *J. R. Stat. Soc., Ser. B* **1995**, *57*, 289−300.
(60) Salek, R. M.; Steinbeck, C.; Viant, M. R.; Goodacre, R.; Dunn, W. B. The Role of Reporting Standards for Metabolite Annotation and Identification in Metabolomic Studies. *Gigascience* **2013**, *2*, No. 13.
(61) Considine, E.; Salek, R. A Tool to Encourage Minimum Reporting Guideline Uptake for Data Analysis in Metabolomics. *Metabolites* **2019**, *9*, No. 43.
(62) Mackay, A. R.; Ballin, M.; Pelina, M. D.; Farina, A. R.; Nason, A. M.; Hartzler, J. L.; Thorgeirsson, U. P. Effect of Phorbol Ester and Cytokines on Matrix Metalloproteinase and Tissue Inhibitor of Metalloproteinase Expression in Tumor and Normal Cell Lines. *Invasion Metastasis* **1992**, *12*, 168−184.
(63) Brama, P. A. J.; Boom, R.; DEGroot, J.; Kiers, G. H.; Weeren, P. R. Collagenase-1 (MMP-1) Activity in Equine Synovial Fluid: Influence of Age, Joint Pathology, Exercise and Repeated Arthrocentesis. *Equine Vet. J.* **2004**, *36*, 34−40.
(64) van den Boom, R.; van der Harst, M. R.; Brommer, H.; Brama, P. A. J.; Barneveld, A.; van Weeren, P. R.; De Groot, J. Relationship between Synovial Fluid Levels of Glycosaminoglycans, Hydroxyproline and General MMP Activity and the Presence and Severity of Articular Cartilage Change on the Proximal Articular Surface of P1. *Equine Vet. J.* **2005**, *37*, 19−25.
(65) Tseng, S.; Reddi, A. H.; Di Cesare, P. E. Cartilage Oligomeric Matrix Protein (COMP): A Biomarker of Arthritis. *Biomark. Insights* **2009**, *4*, 33−44.
(66) Svala, E.; Löfgren, M.; Sihlbom, C.; Rüetschi, U.; Lindahl, A.; Ekman, S.; Skiöldebrand, E. An Inflammatory Equine Model Demonstrates Dynamic Changes of Immune Response and Cartilage Matrix Molecule Degradation in Vitro. *Connect. Tissue Res.* **2015**, *56*, 315−325.
(67) Balakrishnan, L.; Nirujogi, R. S.; Ahmad, S.; Bhattacharjee, M.; Manda, S. S.; Renuse, S.; Kelkar, D. S.; Subbannayya, Y.; Raju, R.; Goel, R.; et al. Proteomic Analysis of Human Osteoarthritis Synovial Fluid. *Clin. Proteomics* **2014**, *11*, No. 6.
(68) Taylor, S. E.; Weaver, M. P.; Pitsillides, A. A.; Wheeler, B. T.; Wheeler-Jones, C. P. D.; Shaw, D. J.; Smith, R. K. W. Cartilage Oligomeric Matrix Protein and Hyaluronan Levels in Synovial Fluid from Horses with Osteoarthritis of the Tarsometatarsal Joint Compared to a Control Population. *Equine Vet. J.* **2006**, *38*, 502−507.
(69) Stashak, T. S.; Theoret, C. *Equine Wound Management*; John Wiley & Sons, 2011.
(70) Peffers, M. J. Proteomic and Transcriptomic Signatures of Cartilage Ageing and Disease, Ph.D. Thesis, University of Liverpool, 2013.
(71) Lust, G.; Burton-Wurster, N.; Leipold, H. Fibronectin as a Marker for Osteoarthritis. *J. Rheumatol.* **1987**, *14 Spec No*, 28−29.

https://dx.doi.org/10.1021/acs.jproteome.0c00143
J. Proteome Res. 2020, 19, 3652−3667

(72) Murray, R. C.; Janicke, H. C.; Henson, F. M.; Goodship, A. Equine Carpal Articular Cartilage Fibronectin Distribution Associated with Training, Joint Location and Cartilage Deterioration. *Equine Vet. J.* **2000**, *32*, 47−51.
(73) Burridge, K.; Wennerberg, K. Rho and Rac Take Center Stage. *Cell* **2004**, *116*, 167.
(74) Woods, A.; Wang, G.; Beier, F. RhoA/ROCK Signaling Regulates Sox9 Expression and Actin Organization during Chondrogenesis. *J. Biol. Chem.* **2005**, *280*, 11626−11634.
(75) Wang, G.; Woods, A.; Sabari, S.; Pagnotta, L.; Stanton, L. A.; Beier, F. RhoA/ROCK Signaling Suppresses Hypertrophic Chondrocyte Differentiation. *J. Biol. Chem.* **2004**, *279*, 13205−13214.
(76) Wang, K.; Kwan, E.; Aris, K.; Egelhoff, T.; Caplan, A.; Welter, J.; Baskaran, H. The Effect of RhoA/ROCK Signaling Inhibition on the Development of HMSC-Based Chondrogenic Tissue. *Osteoarthritis Cartilage* **2017**, *25*, S77.
(77) Deng, Z.; Jia, Y.; Liu, H.; He, M.; Yang, Y.; Xiao, W.; Li, Y. RhoA/ROCK Pathway: Implication in Osteoarthritis and Therapeutic Targets. *Am. J. Transl. Res.* **2019**, 5324−5331.
(78) Shikhman, A. R.; Brinson, D. C.; Valbracht, J.; Lotz, M. K. Cytokine Regulation of Facilitated Glucose Transport in Human Articular Chondrocytes. *J. Immunol.* **2001**, *167*, 7001−7008.
(79) Hernvann, A.; Jaffray, P.; Hilliquin, P.; Cazalet, C.; Menkes, C.-J.; Ekindjian, O. G. Interleukin-1β-Mediated Glucose Uptake by Chondrocytes. Inhibition by Cortisol. *Osteoarthritis Cartilage* **1996**, *4*, 139−142.
(80) Lee, J. Y.; Kang, M. J.; Choi, J. Y.; Park, J. S.; Park, J. K.; Lee, E. Y.; Lee, E. B.; Pap, T.; Yi, E. C.; Song, Y. W. Apolipoprotein B Binds to Enolase-1 and Aggravates Inflammation in Rheumatoid Arthritis. *Ann. Rheum. Dis.* **2018**, 1480.
(81) Sánchez-Enríquez, S.; Torres-Carrillo, N. M.; Vázquez-Del Mercado, M.; Salgado-Goytia, L.; Rangel-Villalobos, H.; Muñoz-Valle, J. F. Increase Levels of Apo-A1 and Apo B Are Associated in Knee Osteoarthritis: Lack of Association with VEGF-460 T/C and +405 C/G Polymorphisms. *Rheumatol. Int.* **2008**, *29*, 63−68.
(82) Lamers, R.-J. A. N.; DeGroot, J.; Spies-Faber, E. J.; Jellema, R. H.; Kraus, V. B.; Verzijl, N.; TeKoppele, J. M.; Spijksma, G. K.; Vogels, J. T. W. E.; van der Greef, J.; et al. Identification of Disease- and Nutrient-Related Metabolic Fingerprints in Osteoarthritic Guinea Pigs. *J. Nutr.* **2003**, *133*, 1776−1780.
(83) Strzelecka-Kiliszek, A.; Mebarek, S.; Roszkowska, M.; Buchet, R.; Magne, D.; Pikula, S. Functions of Rho Family of Small GTPases and Rho-Associated Coiled-Coil Kinases in Bone Cells during Differentiation and Mineralization. *Biochim. Biophys. Acta, Gen. Subj.* **2017**, 1009.
(84) Catalano, M.; O'Driscoll, L. Inhibiting Extracellular Vesicles Formation and Release: A Review of EV Inhibitors. *J. Extracell. Vesicles* **2020**, *9*, No. 1703244.
(85) Li, Z.; Wang, Y.; Xiao, K.; Xiang, S.; Li, Z.; Weng, X. Emerging Role of Exosomes in the Joint Diseases. *Cell. Physiol. Biochem.* **2018**, 2008−2017.
(86) Withrow, J.; Murphy, C.; Liu, Y.; Hunter, M.; Fulzele, S.; Hamrick, M. W. Extracellular Vesicles in the Pathogenesis of Rheumatoid Arthritis and Osteoarthritis. *Arthritis Res. Ther.* **2016**, No. 286.
(87) Zhang, W.; Sun, G.; Likhodii, S.; Liu, M.; Aref-Eshghi, E.; Harper, P. E.; Martin, G.; Furey, A.; Green, R.; Randell, E.; et al. Metabolomic Analysis of Human Plasma Reveals That Arginine Is Depleted in Knee Osteoarthritis Patients. *Osteoarthritis Cartilage* **2016**, *24*, 827−834.
(88) Hu, T.; Oksanen, K.; Zhang, W.; Randell, E.; Furey, A.; Sun, G.; Zhai, G. An Evolutionary Learning and Network Approach to Identifying Key Metabolites for Osteoarthritis. *PLoS Comput. Biol.* **2018**, *14*, No. e1005986.
(89) Abramson, S. B. Osteoarthritis and Nitric Oxide. *Osteoarthritis Cartilage* **2008**, *16*, S15−S20.
(90) Loeser, R. F.; Carlson, C. S.; Del Carlo, M.; Cole, A. Detection of Nitrotyrosine in Aging and Osteoarthritic Cartilage: Correlation of Oxidative Damage with the Presence of Interleukin-1? And with Chondrocyte Resistance to Insulin-like Growth Factor 1. *Arthritis Rheum.* **2002**, *46*, 2349−2357.
(91) Ivaska, J.; Pallari, H.-M.; Nevo, J.; Eriksson, J. E. Novel Functions of Vimentin in Cell Adhesion, Migration, and Signaling. *Exp. Cell Res.* **2007**, *313*, 2050−2062.
(92) Langelier, E.; Suetterlin, R.; Hoemann, C. D.; Aebi, U.; Buschmann, M. D. The Chondrocyte Cytoskeleton in Mature Articular Cartilage: Structure and Distribution of Actin, Tubulin, and Vimentin Filaments. *J. Histochem. Cytochem.* **2000**, *48*, 1307−1320.
(93) Lambrecht, S.; Verbruggen, G.; Verdonk, P. C. M.; Elewaut, D.; Deforce, D. Differential Proteome Analysis of Normal and Osteoarthritic Chondrocytes Reveals Distortion of Vimentin Network in Osteoarthritis. *Osteoarthritis Cartilage* **2008**, *16*, 163−173.
(94) Zhai, G.; Wang-Sattler, R.; Hart, D. J.; Arden, N. K.; Hakim, A. J.; Illig, T.; Spector, T. D. Serum Branched-Chain Amino Acid to Histidine Ratio: A Novel Metabolomic Biomarker of Knee Osteoarthritis. *Ann. Rheum. Dis.* **2010**, *69*, 1227−1231.
(95) Phang, J. M.; Liu, W.; Hancock, C. N.; Fischer, J. W. Proline Metabolism and Cancer: Emerging Links to Glutamine and Collagen. *Curr. Opin. Clin. Nutr. Metab. Care* **2015**, *18*, 71−77.
(96) Milner, J. M.; Elliott, S.-F.; Cawston, T. E. Activation of Procollagenases Is a Key Control Point in Cartilage Collagen Degradation: Interaction of Serine and Metalloproteinase Pathways. *Arthritis Rheum.* **2001**, *44*, 2084−2096.
(97) Milner, J. M.; Rowan, A. D.; Cawston, T. E.; Young, D. A. Metalloproteinase and Inhibitor Expression Profiling of Resorbing Cartilage Reveals Pro-Collagenase Activation as a Critical Step for Collagenolysis. *Arthritis Res. Ther.* **2006**, *8*, No. R142.
(98) Gupta, S.; Biswas, A.; Akhter, M. S.; Krettler, C.; Reinhart, C.; Dodt, J.; Reuter, A.; Philippou, H.; Ivaskevicius, V.; Oldenburg, J. Revisiting the Mechanism of Coagulation Factor XIII Activation and Regulation from a Structure/Functional Perspective. *Sci. Rep.* **2016**, *6*, No. 30105.
(99) Johnson, K.; Hashimoto, S.; Lotz, M.; Pritzker, K.; Terkeltaub, R. Interleukin-1 Induces pro-Mineralizing Activity of Cartilage Tissue Transglutaminase and Factor XIIIa. *Am. J. Pathol.* **2001**, *159*, 149−163.
(100) Sanchez, C.; Deberg, M. A.; Bellahcène, A.; Castronovo, V.; Msika, P.; Delcour, J. P.; Crielaard, J. M.; Henrotin, Y. E. Phenotypic Characterization of Osteoblasts from the Sclerotic Zones of Osteoarthritic Subchondral Bone. *Arthritis Rheum.* **2008**, *58*, 442−455.
(101) Day, J. S.; Van Der Linden, J. C.; Bank, R. A.; Ding, M.; Hvid, I.; Sumner, D. R.; Weinans, H. Adaptation of Subchondral Bone in Osteoarthritis. *Biorheology* **2004**, *41*, 359−368.
(102) Nurminskaya, M.; Magee, C.; Nurminsky, D.; Linsenmayer, T. F. Plasma Transglutaminase in Hypertrophic Chondrocytes: Expression and Cell-Specific Intracellular Activation Produce Cell Death and Externalization. *J. Cell Biol.* **1998**, *142*, 1135−1144.
(103) Rosenthal, A. K.; Masuda, I.; Gohr, C. M.; Derfus, B. A.; Le, M. The Transglutaminase, Factor XIIIA, Is Present in Articular Chondrocytes. *Osteoarthritis Cartilage* **2001**, *9*, 578−581.
(104) Roughley, P. J.; White, R. J.; Cs-Szabó, G.; Mort, J. S. Changes with Age in the Structure of Fibromodulin in Human Articular Cartilage. *Osteoarthritis Cartilage* **1996**, *4*, 153−161.
(105) Wadhwa, S.; Embree, M. C.; Kilts, T.; Young, M. F.; Ameye, L. G. Accelerated Osteoarthritis in the Temporomandibular Joint of Biglycan/Fibromodulin Double-Deficient Mice. *Osteoarthritis Cartilage* **2005**, *13*, 817−827.
(106) Ameye, L.; Aria, D.; Jepsen, K.; Oldberg, A.; Xu, T.; Young, M. F. Abnormal Collagen Fibrils in Tendons of Biglycan/Fibromodulin-Deficient Mice Lead to Gait Impairment, Ectopic Ossification, and Osteoarthritis. *FASEB J.* **2002**, *16*, 673−680.
(107) Swift, J.; Discher, D. E. The Nuclear Lamina Is Mechano-Responsive to ECM Elasticity in Mature Tissue. *J. Cell Sci.* **2014**, *127*, 3005−3015.
(108) Attur, M.; Ben-Artzi, A.; Yang, Q.; Al-Mussawir, H. E.; Worman, H. J.; Palmer, G.; Abramson, S. B. Perturbation of Nuclear

https://dx.doi.org/10.1021/acs.jproteome.0c00143
J. Proteome Res. 2020, 19, 3652−3667

Lamin A Causes Cell Death in Chondrocytes. *Arthritis Rheum.* **2012**, *64*, 1940−1949.
(109) Lopez de Figueroa, P.; Nogueira-Recalde, U.; Osorio, F.; Lotz, M.; Lopez-Otin, C.; Blanco, F. J.; Carames, B. Deficient Autophagy Induces Lamin a/C Accumulation in Aging and Osteoarthritis. *Arthritis Rheumatol.* **2017**, *69*.
(110) Lotz, M.; Martel-Pelletier, J.; Christiansen, C.; Brandi, M.-L.; Bruyère, O.; Chapurlat, R.; Collette, J.; Cooper, C.; Giacovelli, G.; Kanis, J. A.; et al. Value of Biomarkers in Osteoarthritis: Current Status and Perspectives. *Ann. Rheum. Dis.* **2013**, *72*, 1756−1763.
(111) Simó, R.; Barbosa-Desongles, A.; Lecube, A.; Hernandez, C.; Selva, D. M. Potential Role of Tumor Necrosis Factor-a in Downregulating Sex Hormone-Binding Globulin. *Diabetes* **2012**, *61*, 372−382.
(112) Hazuda, D. J.; Lee, J. C.; Young, P. R. The Kinetics of Interleukin 1 Secretion from Activated Monocytes. Differences between Interleukin 1α and Interleukin 1β. *J. Biol. Chem.* **1988**, *263*, 8473−8479.
(113) Marshall, D. D.; Powers, R. Beyond the Paradigm: Combining Mass Spectrometry and Nuclear Magnetic Resonance for Metabolomics. *Prog. Nucl. Magn. Reson. Spectrosc.* **2017**, *100*, 1−16.
(114) Parker, C. E.; Borchers, C. H. Mass Spectrometry Based Biomarker Discovery, Verification, and Validation - Quality Assurance and Control of Protein Biomarker Assays. *Mol. Oncol.* **2014**, *8*, 840−858.
(115) Caterson, B.; Baker, J. R.; Christnerg, J. E.; Leell, Y.; Lentzn, M. Monoclonal Antibodies as Probes for Determining the Microheterogeneity of the Link Proteins of Cartilage Proteoglycan. *J. Biol. Chem.* **1985**, *260*, 11348−11356.

https://dx.doi.org/10.1021/acs.jproteome.0c00143
J. Proteome Res. 2020, 19, 3652−3667